

LAPPEENRANTA UNIVERSITY OF TECHNOLOGY
LUT School of Energy Systems
Degree Programme in Energy Technology

Krasulin Sergey

**Development of laboratory exercises for basic nuclear thermal
hydraulics measurements**

Examiners: Prof. D.Sc. Juhani Hyvärinen
M.Sc. (Tech.) Joonas Telkkä
M.Sc. (Tech.) Eetu Kotro

ABSTRACT

Lappeenranta University of Technology
LUT School of Energy Systems
Degree Programme in Energy Technology

Krasulin Sergey

Development of laboratory exercises for basic nuclear thermal hydraulics measurements

Master's thesis

2016

82 pages, 50 figures, 3 tables and 2 appendices

Examiners: Prof. D.Sc. Juhani Hyvärinen
M.Sc. (Tech.) Joonas Telkkä
M.Sc. (Tech.) Eetu Kotro

Keywords: Light Water Reactor, Pressurized Water Reactor, Boiling Water Reactor, measurement, temperature, pressure, fluid level, flow rate.

The thesis focuses on light water reactors (pressurized water reactors, boiling water reactors) and measurement techniques for basic thermal hydraulics parameters that are used in a nuclear power plant. The goal of this work is a development of laboratory exercises for basic nuclear thermal hydraulics measurements.

CONTENTS

1 INTRODUCTION	7
2 LIGHT WATER REACTORS	8
2.1 Pressurized water reactors.....	8
2.2 Boiling Water Reactors.....	12
3 THERMAL HYDRAULICS OF LIGHT WATER REACTORS	14
3.1 Forced convection and natural circulation.....	14
3.1.1 One-phase NC.....	15
3.1.2 Two-phase NC	16
3.1.3 Reflux condensation.....	16
3.2 One-phase and two-phase friction	17
3.2.1 One phase friction	17
3.2.2 Two-phase friction	19
3.3 Critical flow	21
3.4 Flooding (counter current flow)	23
3.5 Boiling. Critical heat flux.....	24
3.6 Condensation.....	27
4 MEASUREMENT TECHNIQUES	30
4.1 Temperature measurements	30
4.1.1 Resistance thermometers	30
4.1.2 Thermoelectric temperature sensor	34
4.2 Pressure and pressure difference measurements	39
4.2.1 Piezoelectric converters	39
4.2.2 Piezoresistive strain gauge	40
4.2.3 Capacitive pressure sensors	43
4.3 Level measurements.....	45
4.3.1 D/p level transmitters	45
4.3.2 Float level indicator	48
4.3.3 Buoyancy level transmitter	49
4.3.4 Capacitive level indicators	51
4.4 Flow rate measurements.....	56
4.4.1 Variable-pressure drop method	56
4.4.2 Velocity flowmeters	59
4.4.3 Magnetic flowmeters	62
5 DESCRIPTIONS OF LABORATORY SESSIONS	65
5.1 Laboratory session №1: Natural Circulation Test Rig.....	66
5.1.1 Level measurements.....	68
5.1.2 Temperature measurements	70
5.1.3 Flow rate measurements	71
5.1.4 Data processing.....	72
5.1.5 Friction factor calculation	73
5.2 Laboratory session №2: Horizontal and Inclined Pipe flow Experiments.....	75

5.2.1 Preliminary exercises	76
5.2.2 Performance	77
5.2.3 Data processing	78
6 SUMMARY	79
References.....	80

Appendix A. "Study guidance of natural circulation test rig laboratory session"

Appendix B. "Study guidance of Horizontal and Inclined Pipe flow experiments laboratory session"

Nomenclature

Roman

c	spring stiffness
C	discharge coefficient
C	electrical capacitance
d	diameter
D	diameter
E	velocity factor
E	electromotive force
f	cross-sectional area
F	cross-sectional area
F	force
g	gravitation constant
G	flow rate
G	force of gravity
h	level of the liquid
h	heat transfer coefficient
H	level of the liquid
H	heat transfer coefficient
I	electrical current
k	pressure gauge constant
p	pressure
Q	electrical charge
R	resistance
Re	Reynolds number
S	area
t	temperature
u	voltage
V	volume
x	coordinate
Z	total resistance

Greek

α	share
α	temperature coefficient
β	relative diameter
ε	expansion factor
Δp	pressure difference
Δu	voltage difference
ε	dielectric constant
ρ	density
λ	heat-conduction coefficient

Subscripts

0	0 °C temperature
0	free ends
a	absolute
at	atmospheric
b	balanced
c	compensation
fb	feedback
f	film
g	gas
g	gage
i	insulator
l	liquid
l	load
m	mass
r	radial
r	reservoir
t	temperature
v	volumetric
w	water
τ	shear

List of Acronyms

A	Amplifier
BWR	Boiling Water Reactor
EMF	Electromotive Force
FD	Feedback Device
LWR	Light Water Reactor
M	Multiplier
NC	Natural Circulation
NT	Normalizing Transducer
PWR	Pressurized Water Reactor
RTD	Resistance Temperature Detector
SA	Synchronization Annunciator
SG	Steam Generator
SI	Secondary Instrument

1 INTRODUCTION

Year on year nuclear power engineering is developed further, and share of nuclear energy rises in many countries of the world. New nuclear units and nuclear power plants (NPPs) under construction and modernization prove that fact.

A major part of nuclear power plants are nuclear reactors which produce thermal energy from nuclear fission for a steam generation. Steam rotates turbine with the generator producing electrical energy. Different kinds of technologies are used to produce nuclear energy. Generally, there are fast and thermal reactors. The latter have become the most widespread. There are many kinds of thermal reactors with different methods of neutron's moderation and the most common reactors today are light water reactors.

Nuclear power plant is a complex system that consists of variety of technical equipment, which must meet the strictest requirements in reliability, safety and efficiency. For safe and efficient control of NPP operation automated systems are used that contain plenty of measurement instruments: temperature, flow rate, level and pressure sensors and others.

The goal of this master's thesis is a development of laboratory exercises of thermal hydraulics measurements: temperature, pressure, pressure difference, fluid level and flow rate. Laboratory sessions are going to be conducted as a part of intensive course "Experimental nuclear thermal hydraulics" in the School of Energy Systems, Lappeenranta University of Technology.

2 LIGHT WATER REACTORS

The most widespread type of the reactor is a thermal reactor which uses ordinary water as a moderator and as a coolant. Water has significant advantages: its properties are well studied and have shown that water is an excellent moderator. In addition, high availability and low cost promote the light water to be widely used. Nevertheless, water has also disadvantages. Operation of the light-water reactor (LWR) has to be at a high pressure because of high vapor pressure. Besides, as water absorbs thermal neutrons, it is impossible for the LWR using natural uranium to reach criticality. That means fuel enrichment is required. There are two main types of light-water reactors: the pressurized-water reactors (PWR) and the boiling-water reactors (BWR). (Lamarsh J.R. and Baratta A.J., 2001, 137.)

2.1 Pressurized water reactors

A PWR type of nuclear power plant consists of two circuits: a primary circuit and a secondary circuit. The pressure vessel of typical PWR is shown in Figure 1. Inlet water with a temperature 265 - 290 °C flows down along the wall of the reactor core serving as a reflector, goes up through the core, where it is heated up to 300-325 °C. Pressure inside the vessel is maintained at 12.5-16.5 MPa so that the water does not boil. Local boiling is possible. (Lamarsh J.R. Baratta A.J. 2001, 137.)

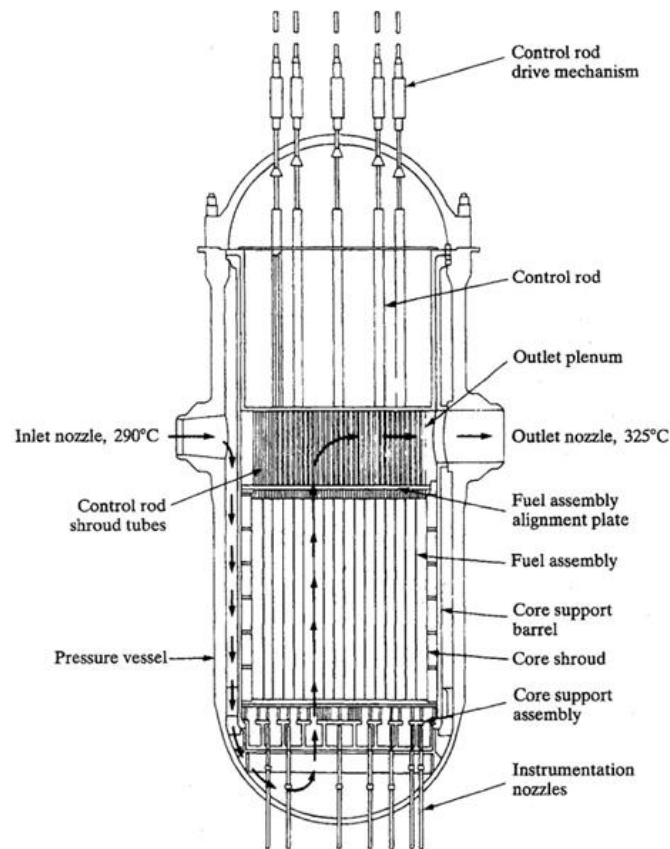


Figure 1. Cross-sectional view of the PWR reactor pressure vessel. (Lamarsh J.R. and Baratta A.J., 2001, 138.)

To produce steam for the turbine steam generators are used. A steam generator is a heat exchanger in which heat is transferred from water of primary circuit to the water of secondary circuit. (Lamarsh J.R. and Baratta A.J. 2001, 137.)

Figure 2 shows a typical steam generator. Pictured is a vertical U-tube generator. There are also straight-tube steam generators and horizontal steam generators manufactured. The coolant heated in the reactor enters the steam generator at the bottom, flows upward and then downward through the tubes and heats the water flowing outside the tubes. This causes boiling because pressure of the secondary circuit is significantly lower than pressure of the primary circuit. The wet steam passes through moisture separators and steam dryers and then the dry steam goes to the turbine. (Lamarsh J.R. and Baratta A.J., 2001, 137-139.)

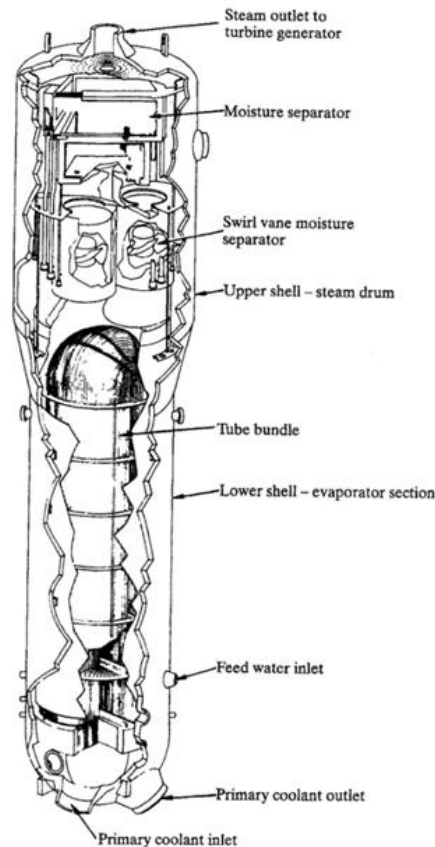


Figure 2. A PWR U-tube steam-generator. (Lamarsh J.R. and Baratta A.J., 2001, 139.)

The pressurizer (Figure 3) is used to control the pressure of the PWR primary circuit. The pressurizer consists of a tank with water in its lower part and steam in the upper part. In case of rising temperature in the system, increasing water level inside the pressurizer raises the steam pressure. Water from the cold leg of the primary circuit through the spray-nozzles condenses some steam to reduce the pressure. In another situation, when water level drops down and pressure in the pressurizer is decreased, electrical heaters limit the pressure reduction. (Lamarsh J.R. and Baratta A.J., 2001, 140.)

Other functions of the pressurizer are monitoring of the water level in the primary circuit, providing a cushion for sudden pressure changes, providing a cushion for sudden pressure changes and providing an over-pressure relief system. (Lamarsh J.R. and Baratta A.J., 2001, 140.)

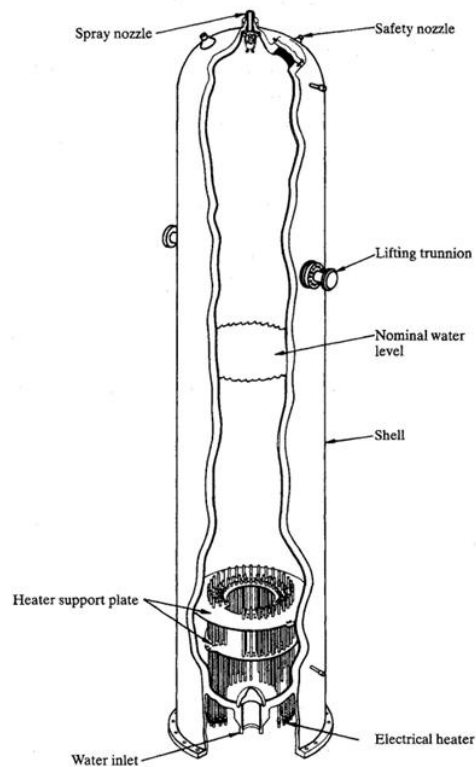


Figure 3. A PWR Pressurizer. (Lamarsh J.R. and Baratta A.J. 2001, 141.)

The major components of a four-loop PWR steam supply system are shown in Figure 4. There are four loops with steam generators and coolant pumps and a single pressurizer for the system. (Lamarsh J.R. and Baratta A.J. 2001, 140.)

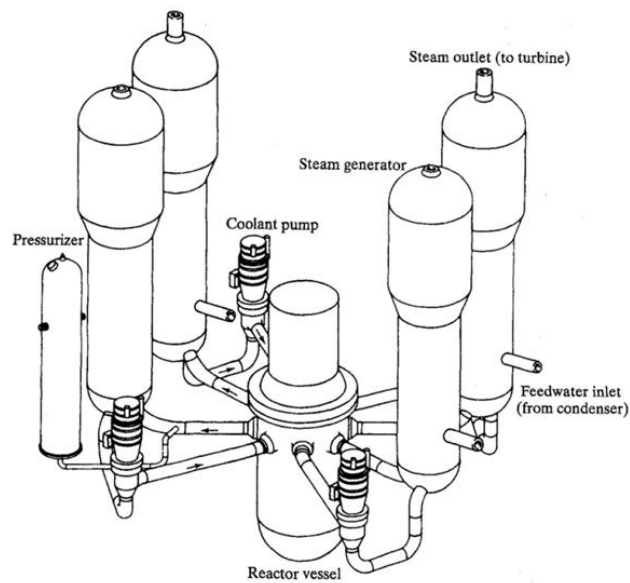


Figure 4. Schematic arrangement of the major components of a PWR steam supply system. (Lamarsh J.R. and Baratta A.J. 2001, 142.)

2.2 Boiling Water Reactors

In difference from the PWR, steam in BWR is generated in the reactor pressure vessel itself and then goes straight to the turbines. That means there is no need for steam generators – secondary loop disappears. Another advantage of the BWR is that less water must be pumped through the reactor than in PWR with the same power. Water in the former can absorb more heat to vaporize water while in the latter it just increases the temperature of the water. On the other hand, the liquid in the cycle is radioactive, so all the equipment that is in a contact with this water must be shielded. (Lamarsh J.R. and Baratta A.J. 2001, 143.)

As boiling-water reactor is operated at a lower pressure (about 7 MPa) than the pressurized-water reactor, walls of the BWR pressure vessel are designed thinner. However, power density is smaller in BWR, so for the BWR with same power as the PWR, larger reactor pressure vessel must be manufactured. Thus, the costs of the reactor pressure vessels of both types are more or less in the same range. In Figure 5 cross-sectional view of the BWR reactor pressure vessel is shown. The water from the lower plenum goes upward through the reactor core receiving heat. As it reaches the upper plenum, part of the water has been vaporized and mixture of steam and water goes through steam separators to remove most of the liquid. After that steam passes through the dryer to remove remaining liquid. (Lamarsh J.R. and Baratta A.J. 2001, 143-146.)

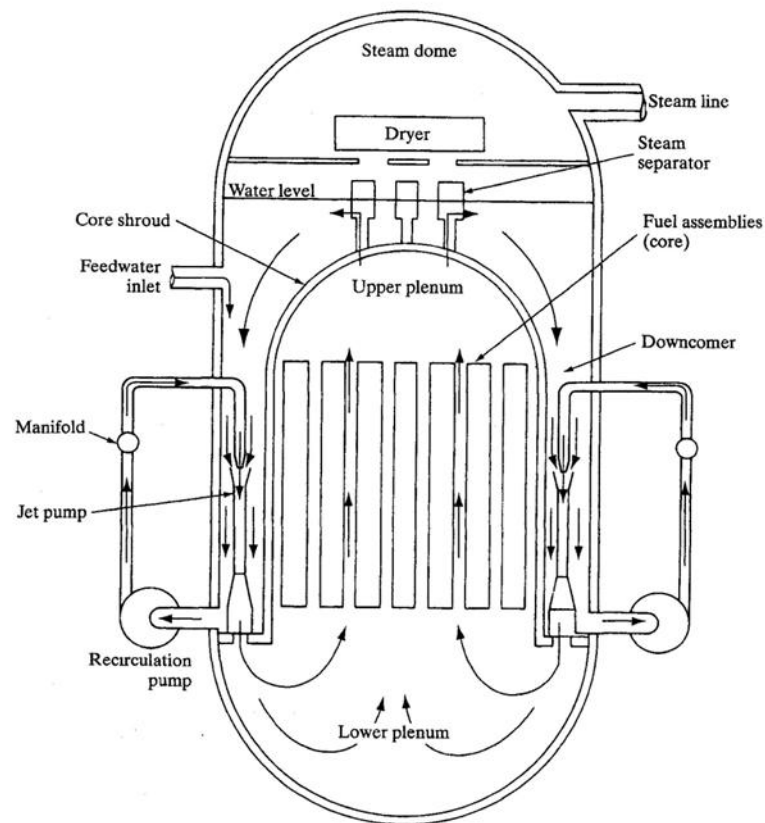


Figure 5. Cross-sectional view of the boiling-water reactor pressure vessel. (Lamarsh J.R. and Baratta A.J. 2001, 145.)

Next the steam moves to the turbine through the steam pipes. The water that has not been vaporized, returns from separators and the dryer and mixes with feed water and flows downward through the downcomer into the lower plenum. (Lamarsh J.R. and Baratta A.J. 2001, 146.)

The recirculation system for pumping the coolant through the core of shown type of BWR contains two loops with one recirculation pump in each. These pumps draw the water from the downcomer and pump it through pipe manifold to a number of jet pumps located within the downcomer. Parameters of the saturated steam produced (temperature about 285-292°C and pressure is 6.8-7.5 MPa) determine the efficiency of the BWR type is 33-34%. (Lamarsh J.R. and Baratta A.J. 2001, 146-147.)

3 THERMAL HYDRAULICS OF LIGHT WATER REACTORS

In previous chapter the main equipment of both types of light water reactors was described. Key flow phenomena presented inside that equipment are listed in Figure 6.

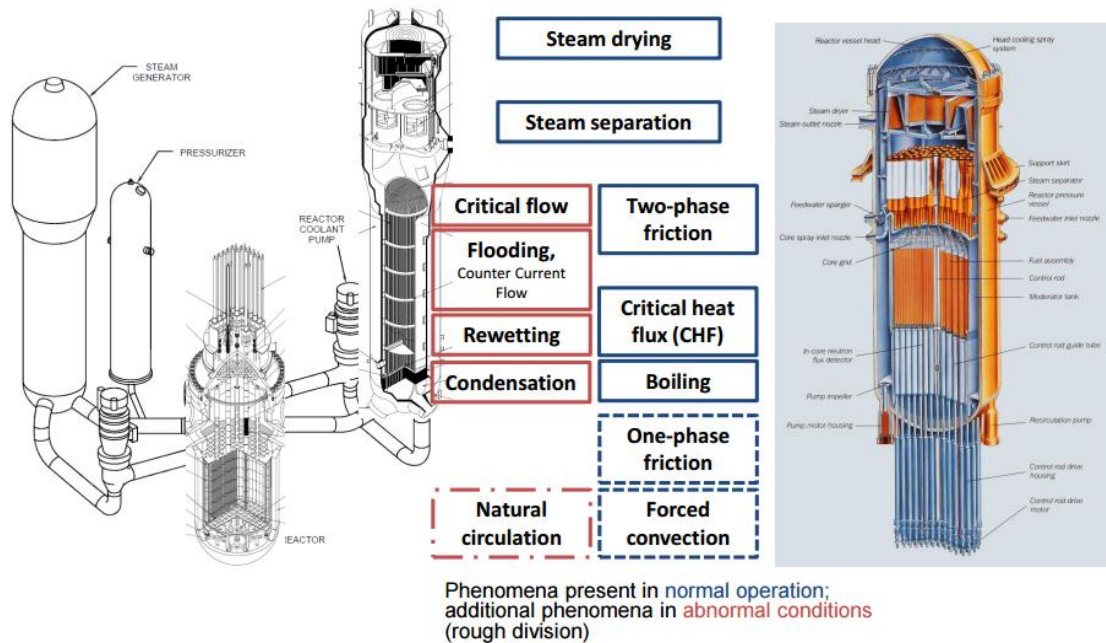


Figure 6. Key flow phenomena in PWRs and BWRs. (Hyvärinen J. 2015, L1-2: 9.)

3.1 Forced convection and natural circulation

In normal operation heat removal from the reactor core is provided by pumping the water through it. In that case the dominant mechanism of heat removal is called forced convection. Forced convection is a process in which flow over the surface or in a tube is initiated by an external pressure gradient such as a fan or a pump. Convective heat transfer involves fluid motion and heat transfer. The higher the velocity of the flow the better is the heat transfer rate. Generally, heat transfer due to forced convection can be described by the expression $Nu = f(Re, Pr)$, where the Nusselt number $Nu = \frac{HD_h}{\lambda}$ is a ratio of convective heat flux at the surface to pure heat conduction in the fluid. Reynolds number $Re = \frac{\rho w D_h}{\mu}$ represents flow inertia divided by shear force due to friction in the fluid and Prandtl number $Pr = \frac{\mu c_p}{\lambda}$ is the ratio of momentum diffusivity to thermal diffusivity. Reynolds number determines a flow regime: laminar or turbulent. For instance, in a channel: flow

with $Re < 2300$ is laminar, $Re > 20000$ is turbulent. (Korotkikh A.G. and Shamanin I.V. 2007, 72.)

The natural circulation (NC) is an important mechanism in nuclear reactor systems and the knowledge of its behavior is of interest to nuclear reactor design, operation, and safety.

Natural circulation mass flow rate is the most interesting parameter, which is a function of reactor power that has to be removed, system pressure and secondary pressure. (Korotkikh A.G. and Shamanin I.V. 2007, 60.)

There are three modes of natural circulation in PWRs: one-phase natural circulation, two-phase natural circulation and reflux condensation.

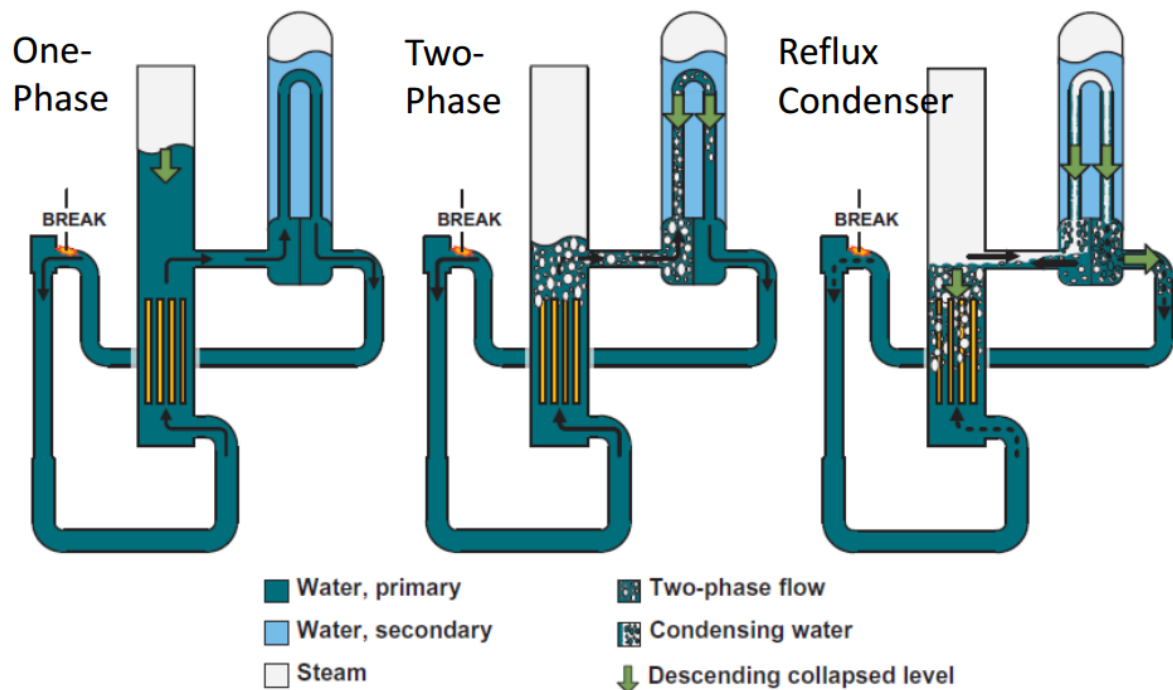


Figure 7. PWR natural circulation modes. (Hyvärinen J. 2015, L9-10: 18.)

3.1.1 One-phase NC

One-phase NC mode means no steam is present in the upper plenum of the system. Water at the outlet of the core is subcooled or almost saturated. Flow rate in the core is calculated from the balance between driving and resistant forces. Driving force appears due to

difference of coolant density occurring between downcoming part of steam generator (SG) tubes and pressure vessel downcomer and core and upcoming part of SG tubes. Resistant forces are determined by irreversible friction pressure losses inside the whole loop. Resulting coolant velocities suffice for cooling the core. It should be noted that the secondary side of steam generator works in two-phase natural circulation regime. (Cherubini M. et al. 2007, 1-2.)

3.1.2 Two-phase NC

Two-phase natural circulation mode appears as a result of loss of coolant accident in the primary circuit. Therefore, resistance and driving forces increase when mass of coolant in primary circuit diminishes. Increase of driving forces is dominant at small inventory losses. Resistive forces appear for larger decreases of mass inventories. Forced convection, subcooled, and saturated heat transfer regimes occur in the core. Condensation appears inside the steam generator pipes. Typically, an average core void fraction is less than 30%, whereas at the outlet values around 50% can be reached without thermal crisis in the considered pressure range. (Cherubini M. et al. 2007, 2.)

3.1.3 Reflux condensation

Reflux condensation in steam generator is one of the major heat removal mechanisms in a hypothetical loss of residual heat removal system event in mid-loop operation during a pressurized water reactor plant outage. In this mode generated steam condenses inside steam generator tubes. Condensate drains back through both the hot leg and the cold leg, and cools the reactor core. When studying the effectiveness of reflux condensation mode, present non-condensable gases should be also taken in to an account, as they have a certain influence. (Nagae T. et al. 2005, 50.)

3.2 One-phase and two-phase friction

3.2.1 One phase friction

Fluid flow in the channel experiences an impact of external forces that change the energy of the flow. Energy losses of the flow are determined by a work of external and internal friction forces. There two kinds of friction losses: pressure losses Δp_l which are uniformly or non-uniformly distributed along the entire length of the flow in dependence of a channel diameter and a flow velocity. And local pressure losses Δp_j which occur only in certain parts of the flow because of a channel configuration change and in flow turns.

Generally, for a section of a pipe full pressure losses can be written as:

$$\Delta p = \Delta p_l + \sum \Delta p_j. \quad (1)$$

For uniform steady flow of real fluid, external forces are always equal to friction forces. As a result of friction forces kinetic energy of the flow transforms into thermal energy.

For pressure losses along a length of a smooth channel Darcy-Weisbach equation applies:

$$\Delta p_l = \xi \frac{l}{D} \frac{v^2}{2g}; \quad (2)$$

This formula is used for both laminar and turbulent single-phase flow. However, friction factor ξ is different. For laminar flow friction factor ξ is calculated:

$$\xi = \frac{64}{Re_D}; \quad (3)$$

For fully developed turbulent flow in smooth channels, Blasius' correlation is used:

$$\xi = \frac{0.3164}{Re_D^{0.25}}; \quad (4)$$

Additional energy losses occur because of turning of the flow and changing geometry of the channel. These losses are called local pressure losses. (Vidyaev D.G. 2009, 47-49.)

Calculation of local pressure losses: sudden expansion and sudden contraction.

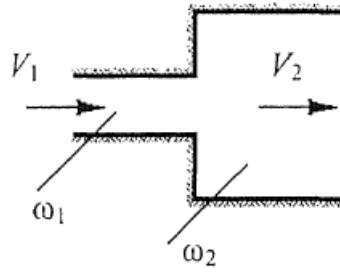


Figure 8. Sudden expansion. (Vidyaev D.G. 2009, 52.)

Pressure loss of sudden expansion includes reversible and irreversible components

$$\Delta p_{\text{Exp}} = \Delta p_{\text{R,Exp}} + \Delta p_{\text{I,Exp}}; \quad (5)$$

$$\Delta p_{\text{R,Exp}} = \frac{1}{2} \rho V_1^2 (\sigma^2 - 1); \quad (6)$$

$$\Delta p_{\text{I,Exp}} = \frac{1}{2} \rho V_1^2 (1 - \sigma)^2, \quad (7)$$

where σ is a ratio of cross-sections $\sigma = \frac{\omega_2}{\omega_1}$

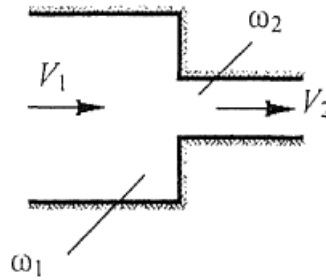


Figure 9. Sudden contraction. (Vidyaev D.G. 2009, 56.)

$$\Delta p_{\text{Con}} = \Delta p_{\text{R,Con}} + \Delta p_{\text{I,Con}}; \quad (8)$$

$$\Delta p_{\text{R,Con}} = \frac{1}{2} \rho V_2^2 (1 - \sigma^2); \quad (9)$$

$$\Delta p_{\text{I,Con}} = K_{\text{Con}} \frac{1}{2} \rho V_2^2; \quad (10)$$

$$K_{\text{Con}} = \left(\frac{1}{C_c} - 1 \right)^2; \quad (11)$$

$$C_c = 1 - \frac{1 - \sigma}{2.08(1 - \sigma) + 0.5371}; \quad (12)$$

(Ghiaasiaan S.M. 2007, 219.)

3.2.2 Two-phase friction

Two-phase flow can be modeled as homogenous flow. In this case, two-phase flow is treated as one phase-flow but fluid properties must be averaged.

$$\left(-\frac{dP}{dz}\right)_{fr} = 4f_{TP} \frac{1}{D_H} \frac{G^2}{2\rho_{TP}}, \quad (13)$$

where Blasius' correlation is used for friction factor:

$$f_{TP} = 0.079 Re_{TP}^{-0.25}; \quad (14)$$

$$Re_{TP} = \frac{GD_h}{\mu_{TP}}; \quad (15)$$

with quality weighted harmonic average of substance properties:

$$\text{Density } \rho_{TP} = \left(\frac{x}{\rho_G} + \frac{1-x}{\rho_L}\right)^{-1}; \quad (16)$$

$$\text{Dynamic viscosity } \mu_{TP} = \left(\frac{x}{\mu_G} + \frac{1-x}{\mu_L}\right)^{-1}; \quad (17)$$

More accurate calculation of pressure losses is possible with two-phase multipliers Φ^2 that represent a ratio between two phase pressure drop and single-phase pressure drop:

$$\left(-\frac{dP}{dz}\right)_{fr} = \Phi_{L0}^2 \left(-\frac{dP}{dz}\right)_{fr,L0} \quad \text{All of mass flux } G \text{ is considered as liquid;}$$

$$\left(-\frac{dP}{dz}\right)_{fr} = \Phi_{G0}^2 \left(-\frac{dP}{dz}\right)_{fr,G0} \quad \text{All of mass flux } G \text{ is considered as gas;}$$

$$\left(-\frac{dP}{dz}\right)_{fr} = \Phi_L^2 \left(-\frac{dP}{dz}\right)_{fr,L} \quad \text{There is only liquid mass flow, } G(1-x)$$

$$\left(-\frac{dP}{dz}\right)_{fr} = \Phi_G^2 \left(-\frac{dP}{dz}\right)_{fr,G} \quad \text{There is only liquid mass flow, } Gx$$

For $\left(-\frac{dP}{dz}\right)_{fr,L0}$, $\left(-\frac{dP}{dz}\right)_{fr,G0}$, $\left(-\frac{dP}{dz}\right)_{fr,L}$, $\left(-\frac{dP}{dz}\right)_{fr,G}$ Blasius' correlation applies.
(Ghiaasiaan S.M. 2007, 209.)

For two-phase multiplier estimation empirical formulas are usually used. One of such solutions was offered by Martinelli and Lockhart. They introduced two parameters:

$$\left\{ \begin{array}{l} \Phi_G^2 = \frac{dP/dz}{(dP/dz)''} \\ \Phi_L^2 = \frac{dP/dz}{(dP/dz)'} \end{array} \right., \quad (18)$$

which are ratios of two-phase flow pressure gradients dP/dz to pressure gradients of liquid or gas flow. Therefore Martinelli parameter:

$$X^2 = \frac{\Phi_G^2}{\Phi_L^2}, \quad (19)$$

For a general case of flow regime Martinelli and Lockhart found two empirical equations:

$$\begin{cases} \Phi_L^2 = 1 + \frac{C}{X} + \frac{1}{X^2}; \\ \Phi_G^2 = 1 + CX + X^2; \end{cases} \quad (20)$$

Coefficient C is tabulated and depends of flow regime combinations of both phases. For instance, if both liquid and gas flows are turbulent, then $C = 20$ and:

$$X_{TT}^2 = \left(\frac{\mu_L}{\mu_G}\right)^{0.25} \left(\frac{1-x}{x}\right)^{1.75} \frac{\rho_G}{\rho_L}, \quad (21)$$

Equations (18) were obtained based on experimental data of mixture of the air with different liquids close to atmospheric pressure, so these formulas in application to various ranges of substance parameters may be significantly inaccurate. (Ghiaasiaan S.M. 2007, 209-211.)

Local pressure drops for two-phase flow are described with complex equations:

Contraction:

$$\Delta p_{con} = \frac{1}{2} \frac{G_1^2}{\rho_f} \left(\left(\frac{1}{C_c} - 1 \right)^2 + (1 - \sigma^2) \right) \left(1 + x \left(\frac{\rho_f}{\rho_g} - 1 \right) \right); \quad (22)$$

Expansion:

$$\Delta p_{Rex} = -\frac{1}{2} G_2^2 (1 - \sigma^2) \left(\frac{x^3}{\alpha^2 \rho_g^2} + \left(\frac{(1-x)^3}{(1-\alpha)^2 \rho_f^2} \right) \right) \left(\frac{x}{\rho_g} + \frac{1-x}{\rho_f} \right)^{-1}; \quad (23)$$

$$\Delta p_{Iex} = \frac{1}{2} \frac{G_2^2}{\rho_f} (1 - \sigma^2) \left(1 + x \left(\frac{\rho_f}{\rho_g} - 1 \right) \right). \quad (24)$$

(Ghiaasiaan S.M. 2007, 222.)

3.3 Critical flow

Critical flow (choked flow) is the maximum possible flow rate at given conditions. For example, we have a reservoir with fluid (gas or mixture) that has parameters p_0, T_0, x_0 (Figure 10).

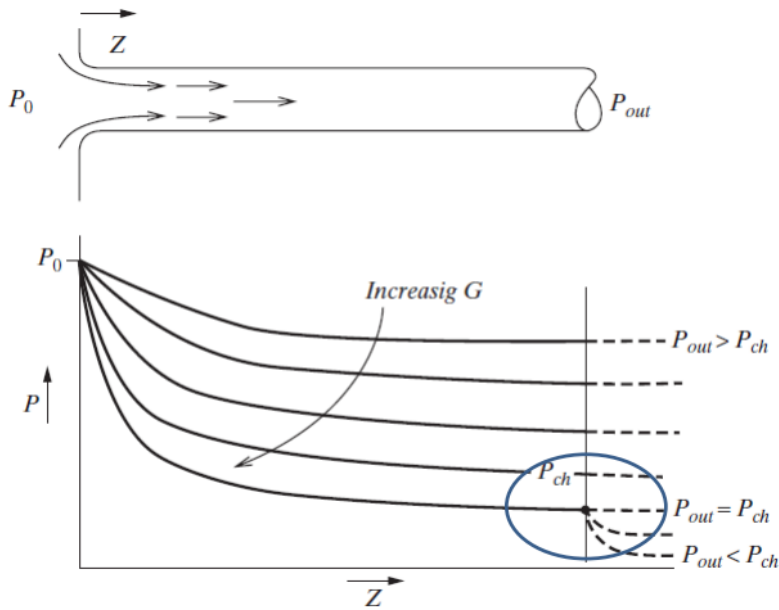


Figure 10. Critical flow illustration. (Ghiaasiaan S.M. 2007, 500.)

Reduction of the outside pressure leads to increase of the flow rate until a certain point (local sonic speed) when further decreasing of p_{out} does not influence the rate through the nozzle and depends only on reservoir conditions. (Ghiaasiaan S.M. 2007, 500.)

Mass flux for single-phase choked flow can be obtained as follows.

Assumptions:

1. flow is adiabatic and frictionless, energy conservation law is $h_0 = h + \frac{1}{2}w^2$;
2. specific heat is constant over temperature range of interest, $h = c_p T$;

$$\text{then mass flux } G = \rho w = \rho \sqrt{2c_p(T_0 - T)} = \rho \sqrt{2c_p T_0 \left(1 - \frac{T}{T_0}\right)}; \quad (25)$$

Using that $pp^{-\gamma} = \text{const}$ and $Tp^{\frac{1-\gamma}{\gamma}} = \text{const}$ (for ideal gases) we get:

$$G = \sqrt{2c_p T_0 \left[\left(\frac{p}{p_0}\right)^{\frac{2}{\gamma}} + \left(\frac{p}{p_0}\right)^{\frac{\gamma+1}{\gamma}} \right]}; \quad (26)$$

Taking in account that outside pressure does not impact on mass flux at choking point:

$$\left(\frac{dG}{dp}\right)_{out} = 0; \quad (27)$$

After differentiating:

$$(p/p_0)_c = \left(\frac{2}{\gamma+1}\right)^{\frac{\gamma}{\gamma-1}}; \quad (28)$$

In the end, mass flux is determined:

$$G_{ch} = \sqrt{2c_p T_0 \left[\left(\frac{2}{\gamma+1}\right)^{\frac{2}{\gamma-1}} + \left(\frac{2}{\gamma+1}\right)^{\frac{\gamma+1}{\gamma-1}} \right]}. \quad (29)$$

(Ghiaasiaan S.M. 2007, 501.)

Two-phase critical flow is much more complex than one-phase critical flow because the amount of liquid phase can quickly change inside the channel. Moreover, different flow regimes are possible depending on steam quality and other factors. The interest in two-phase critical flow is explained with importance of flow rate calculations of two-phase mixture under high pressure. (Derevyanko O.V. et al. 2014, 119.)

As consequence of loss of coolant accident, fuel rod of the nuclear reactor can melt if emergency systems are disabled. Therefore, an accurate estimation of two-phase critical flow is important for the design of emergency core cooling system and damage level prediction in a case of an accident. Homogenous model works at high speed flow, when there is no slip between phases, and thermal equilibrium. (Derevyanko O.V. et al. 2014, 119.)

Assumptions:

- pressure equilibrium is approximate
- densities are only functions of pressure

Then, mass flux can be written:

$$G_{ch} = \left\{ - \left[x \left(\frac{dv_g}{dp} \right) + (1-x) \left(\frac{dv_f}{dp} \right) \right] \right\}^{-\frac{1}{2}} \quad (30)$$

(Ghiaasiaan S.M. 2007, 503.)

There are many models by different authors concerning two-phase critical flow. Each author admits that their assumptions and different models are applicable only for certain cases and parameters of two-phase flow.

3.4 Flooding (counter current flow)

Flooding is an effect when fluid (gas) flow is strong enough to block another fluid (liquid) flow moving in opposite direction (counter current flow) and it can even cause a cocurrent flow. Usually, gas flows upwards and liquid drains downwards as a film in the vertical channel. This phenomenon happens due to interfacial friction and large shear forces which occur under high gas flow rate and cause interfacial waves. Flooding and deflooding processes in vertical pipe are illustrated in Figure 11.

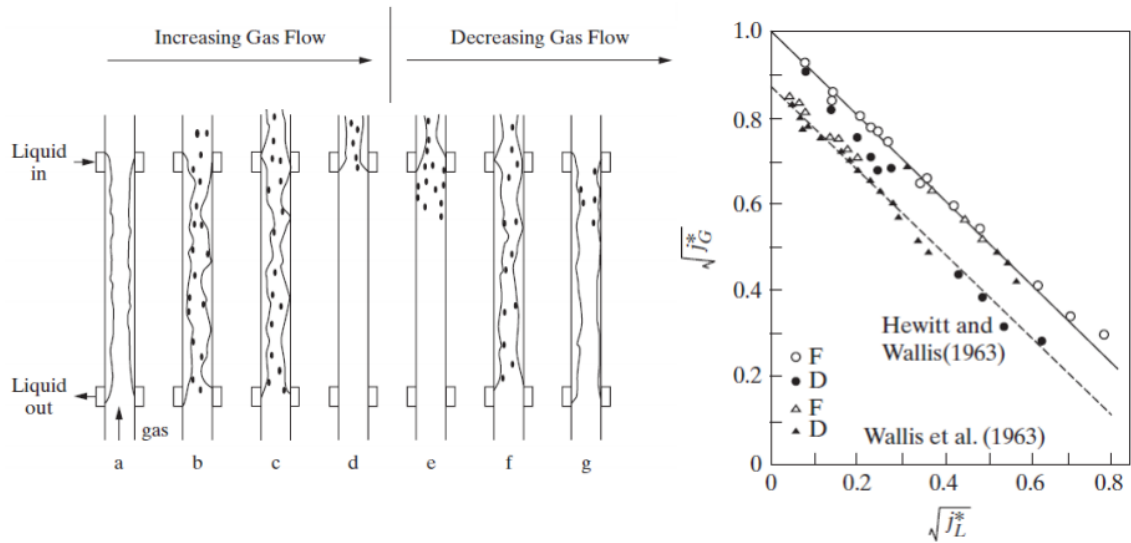


Figure 11. Flooding/deflooding hysteresis in vertical channel. (Hyvärinen J. 2015, L7-8: 42.)

The most widely used correlation for flooding was stated by Wallis:

$$j_G^{*1/2} + m j_L^{*1/2} = C; \quad (31)$$

where j_G^* , j_L^* dimensionless superficial velocities, for most cases $m = 1, C = 1$;

$$j_G^* = \frac{j_G}{\sqrt{\frac{\Delta\rho}{\rho_G} g D}}, j_L^* = \frac{j_L}{\sqrt{\frac{\Delta\rho}{\rho_L} g D}}; \quad (32)$$

Wallis correlation is well applicable for small diameter pipes $2 \leq \frac{D}{\lambda_L} \leq 40$;

$$\lambda_L = \sqrt{\sigma / g \Delta \rho} \quad (33)$$

- Laplace length scale; (Hyvärinen J. 2015, L7-8: 43.)

For large diameter tubes flooding does not depend on diameter anymore. Kutateladze got rid of D and modified Froude number using Laplace length scale to Kutateladze number:

$$K_i^* = \frac{j_i}{\sqrt{\frac{\Delta\rho}{\rho_i} g \sqrt{\sigma/g\Delta\rho}}} = j_i \frac{\rho_i^{1/2}}{(\sigma g \Delta\rho)^{1/4}}; \quad (34)$$

Flooding line:

$$K_G^{*1/2} + m_2 K_L^{*1/2} = C_2, \quad (35)$$

where $m_2 \simeq 1$ and $C_2 = 1.7 - 2$.

All flooding correlations are based on Froude number which is modified, for small dimensions, to Wallis number and, for large dimensions, to Kutateladze number. Parameters of these numbers are found experimentally and strongly depend on the geometry. (Hyvärinen J. 2015, L7-8: 44.)

3.5 Boiling. Critical heat flux

In normal operation at nuclear power plant boiling takes place in BWR fuel bundles along most of the length, subcooled boiling may occur in the hottest part of the PWR fuel bundles and in the secondary side of PWRs steam generator. In abnormal conditions, boiling may happen in the PWRs core and in steam generators, in secondary side of cooling system heat exchangers. (Hyvärinen J. 2015, L3-4: 7.)

Pool boiling is well described with the pool boiling curve (Figure 12). It can be distinguished into five regions:

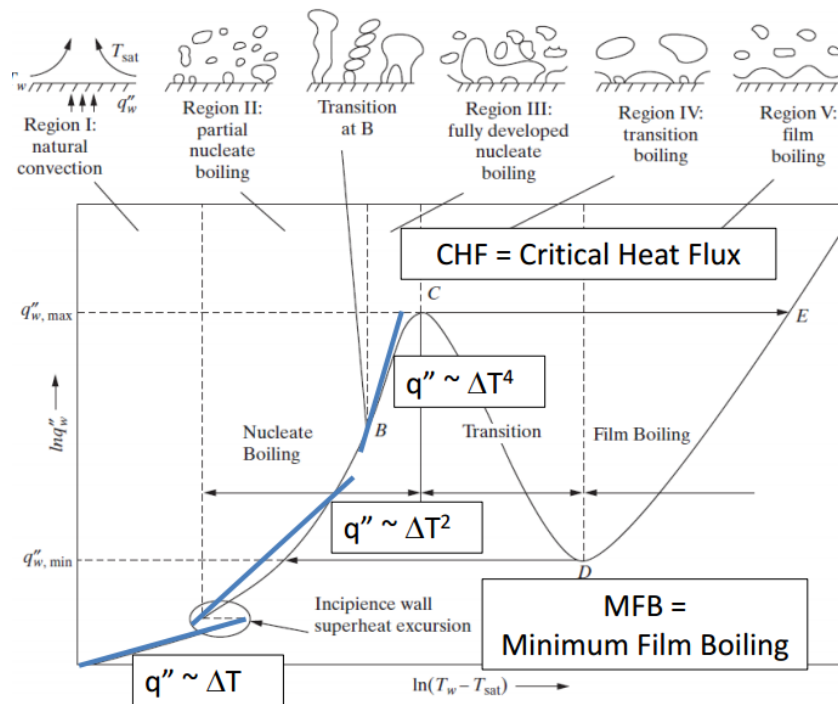


Figure 12. Pool boiling curve. (Ghiaasiaan S.M. 2007, 288.)

Region 1. The region of a single-phase natural convection under small q and ΔT . At this moment, evaporation is not intensive because of the low fluid overheating, therefore, heat removal is provided by natural convection. (Isachenko V.P. et al. 1975, 301-302.)

Region 2 and region 3. These are regions of nucleate boiling. Highly intensive heat exchange determined by pulse-vortexing of fluid with intensive steam bubble generation. (Isachenko V.P. et al. 1975, 301-302.)

Region 4. A strange fact is observed: with temperature difference increase heat flux is decreasing. It is called a transition region between nucleate and film boiling. Transition is possible only if temperature difference is controlled. If heat flux is controlled parameter than increasing q reaches critical heat flux. Critical heat flux (CHF) is a point of the drop from nucleate boiling to film boiling with a temperature drop which usually causes material destruction. It should be noted, that with heat flux decreasing until minimum film boiling (MFB) the same drop from film boiling to nucleate boiling occurs. However, there is a hysteresis and therefore MFB is less than CHF. (Isachenko V.P. et al. 1975, 301-302.)

Region 5. Film boiling. Steam film isolates a hot wall from the fluid because of steam high thermal resistance determined by low thermal conductivity. As a result, heat transfer coefficient at film boiling is much less than at nucleate boiling. (Isachenko V.P. et al. 1975, 301-302.)

Boiling in the vertical channel at moderate heat flux is shown in Figure 13.

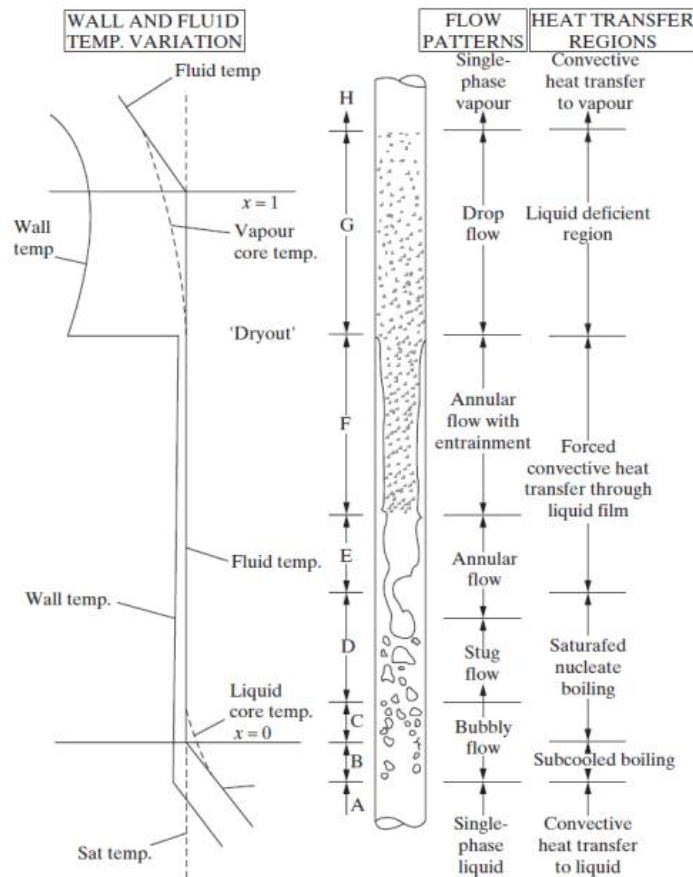


Figure 13. Boiling in the vertical channel at moderate heat flux. (Ghiaasiaan S.M. 2007, 323.)

Here seven flow patterns are presented, which exist between single-phase liquid and single-phase vapor. When liquid film is depleted from the wall, dryout occurs (critical heat flux). However, it is a dangerous point when heat exchange between coolant and wall abruptly gets worse.

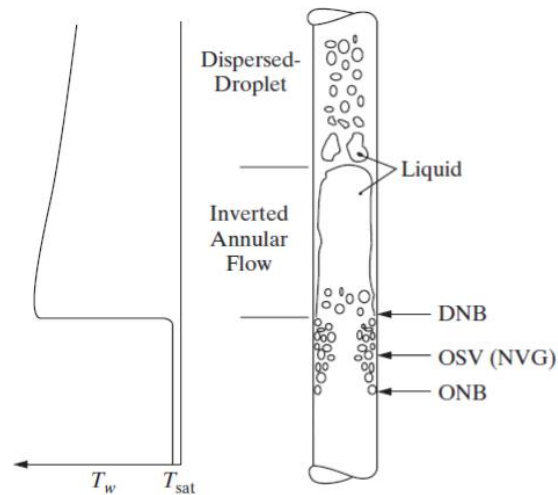


Figure 14. Boiling in the vertical channel at high heat flux. (Hyvärinen J. 2015, L3-4: 14.)

In Figure 14 boiling in the vertical channel at high heat flux is shown, where

DNB – Departure from nucleate boiling;

OSV – Onset of significant void;

NVG – Net vapour generation;

ONB – Onset of nucleate boiling; (Hyvärinen J. 2015, L3-4: 14.)

3.6 Condensation

Condensation is an exoenergetic process of transition from gas phase to liquid phase attended by latent heat generation. In nuclear reactors film condensation appears inside or outside pipes, or condensation occurs as a result of direct contact with fluid in large vessels and suppression pools. (Isachenko V.P. et al. 1975, 263.)

When condensing steam moves inside a channel, flow regimes and the nature of the interaction between vapor and liquid phases can vary as a result of changes in steam velocity, shear stress of friction at the interface and Reynolds number. At high steam velocities (when the effect of gravity on the film of condensate is negligible and film flow is basically determined by friction) local and average heat transfer coefficients over tube length does not depend on space orientation of the pipe. If the gravity and friction forces are comparable, condensation conditions are defined by the tube inclination angle and mutual direction of the phases. In the case of steam condensation inside the horizontal pipe

at low velocity annular flow, condensate film is formed only on the upper part of the inner surface of the tube. On the lower part there is a "stream", therefore in this area, as a result of a relatively large film thickness, heat transfer is much less intensive than in the rest of the surface area. (Isachenko V.P. et al. 1975, 279-281.)

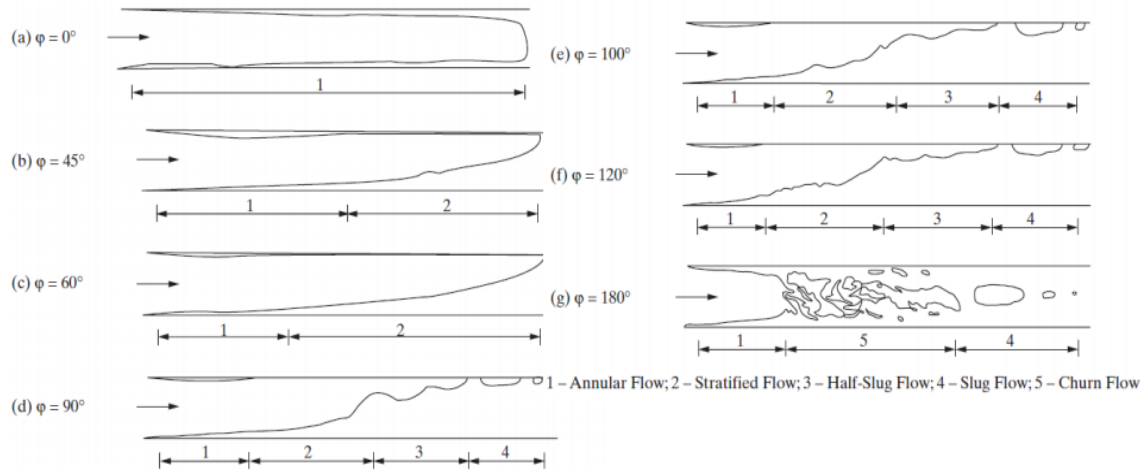


Figure 15. Multiple flow regimes at condensation inside the tube ($\varphi = 0$ is a vertical downward flow).

(Ghiaasiaan S.M. 2007, 463.)

In the case of condensation on the horizontal pipe bank the flow rate of draining condensate increases downwards owing to leakage of condensate from the overlying pipes, and steam flow rate along its path is reduced. The tube bank with a relatively constant or slightly decreasing height over the flow section between pipes downstream flow velocity is gradually reduced, and the condensate drains from the top to bottom pipes. First, it leads to a decrease of the local heat transfer coefficient (averaged over the perimeter of the pipe) by increasing the number counted from the top of the horizontal row of tubes. However, since some row number draining condensate disturbs the film flow and its thermal resistance decreases. Due to this, heat transfer coefficients can be stabilized and, with the increasing influence of the disturbance on the film at lower tubes, they increase with the number of rows. (Isachenko V.P. et al. 1975, 283-284.)

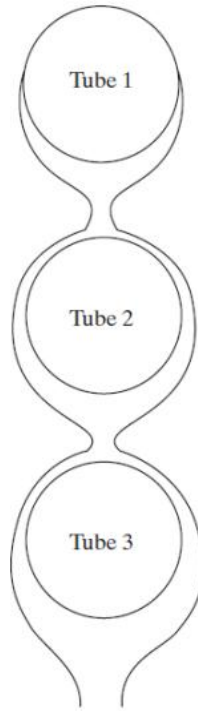


Figure 16. Condensation on the tube bank. (Ghiaasiaan S.M. 2007, 451.)

Correlation of heat transfer coefficient estimation for condensation on horizontal tube (low-velocity steam flow):

$$\overline{Nu}_F = \frac{\overline{H}_F D}{k_L} = 0.728 \left[\frac{g h_{fg} \rho_L (\rho_L - \rho_G) D^3}{\mu_L k_L (T_{sat} - T_W)} \right]^{1/4}; \quad (36)$$

For a bank of n rows:

$$\frac{\overline{Nu}_F}{\overline{Nu}_{F1}} = n^{-\frac{1}{4}}, \quad (37)$$

where \overline{Nu}_{F1} is calculated for the first row. (Hyvärinen J. 2015, L9-10: 8-9.)

4 MEASUREMENT TECHNIQUES

4.1 Temperature measurements

Temperature, volume and pressure are the three basic quantities characterizing the state of matter. Temperature measurement covers 80% of the total industrial measurements. In most cases, temperature determines the quality of products, efficiency of production processes and the safety of the equipment. (Ivanova G.M. et al. 2005, 34.)

Direct measurement of the temperature is impossible. In principle, all the phenomena occurring under the influence of heat can be used to measure temperature. In this section, we will discuss methods of temperature measurements, which are widely used in the nuclear engineering. (Ivanova G.M. et al. 2005, 34.)

4.1.1 Resistance thermometers

Resistance thermometers (RTDs) are one of the most common measurement devices used in measurements and control systems. To measure the temperature, RTD has to be immersed into a substance and its resistance has to be measured. Temperature transmitter is combination of the RTD based on the dependence between an electrical resistance and a temperature, and a secondary device, showing a temperature as a function of the measured resistance. Transmitters usually have a standardized output (e.g. 0...5 V, 0...20 mA or digital signal) (Figure 17). For use in multiple channels, this signal is multiplied and then it goes to a number of secondary instruments. (Gordov A.N. et al. 1992, 55-56.)

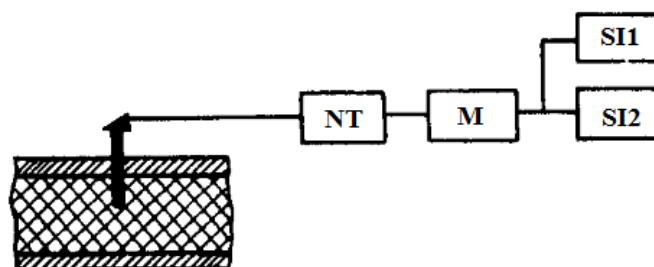


Figure 17. Resistance thermometer. (Ivanova G.M. et al. 2005, 47.)

NT – normalizing transducer, M – multiplier, SI1, SI2 – secondary instruments

For producing RTD either pure metals or semiconductor materials are used. The electrical resistance of pure metals increases with temperature. Semiconductor resistance thermometers have a negative temperature coefficient. Semiconductor resistance thermometers are not used in process control systems for temperature measurement, since they require periodic individual calibration, therefore, we will not discuss them in detail. (Gordov A.N. et al. 1992, 58.)

Resistance thermometers, the most widespread, are usually made of thin wire winding on a frame or spiral inside the frame. This unit is called a sensor. To prevent damage to the sensor it is placed inside a protective tube. Materials of sensors must meet several requirements; the most important are the stability and reproducibility of the calibration curve (i.e. the possibility of mass production of instruments with the same calibration characteristic). Additional requirements are large temperature coefficient of electrical resistance (which provides a high sensitivity), the linearity of the calibration characteristics, high specific electrical resistance and chemical inertness. Resistance thermometers can be made of platinum, copper or nickel. (Ivanova G.M. et al. 2005, 48-49.)

Platinum resistance thermometers

Platinum resistance thermometers may have the following resistance at 0 °C: $R_0 = 1, 5, 10, 50, 100$ and 500 Ohms. Platinum resistance thermometers are used to measure temperature in the range $(-260 \dots 1100)^\circ\text{C}$ and are the most common type of RTD. When selecting the platinum RTD one should use the general principle - low-resistance RTD must be used for the measurement of high temperatures and high-resistance RTD - to measure low temperatures. In addition, when using high-resistance RTD an impact of resistance changes of the external line affects less than using a low-resistance RTD. The disadvantage of platinum RTD is nonlinear static characteristics, especially at high and subzero temperatures, the possibility of contamination of platinum at high temperatures and exposure to reducing and corrosive gases influence. (Gordov A.N. et al. 1992, 60.)

In the temperature range (0...600) °C temperature dependence of resistance is described by a non-linear expression

$$R_t = R_0(1 + At + Bt^2). \quad (38)$$

For the manufacture of RTD platinum wire with a diameter of 0.05 to 0.1 mm (for temperatures up to 750 °C) and a diameter of 0.2 to 0.5 for temperatures up to 1100 °C is used. Standard design of the sensor is shown in Figure 18.

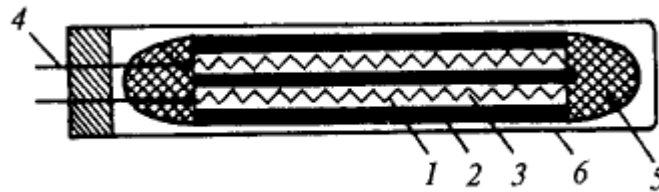


Figure 18. Sensor of the platinum resistance thermometer. (Ivanova G.M. et al. 2005, 53.)

Sensor consists of two series-connected platinum spirals *1* installed in channels of the ceramic frame *2*. The channels are filled with powder *3* (usually magnesium oxide), which serves as a heat conductor and improves the contact of wire with the frame. Short leads of platinum or iridium wire *4* are soldered to junctions of the spirals, to which then isolated terminal conductors are soldered. The ends of ceramic frame are sealed with a special glaze *5*. The frame is placed inside a thin-walled metal shell *6*, which is also filled with powder and closed by a plug which terminals are passed through. The length of platinum sensor is typically 50...100 mm with a diameter 3...6 mm. (Ivanova G.M. et al. 2005, 52-53.)

Copper resistance thermometers

Copper resistance thermometers are used for long-term temperature measurement in a range (-200...200) °C. The advantages of copper as the material for the sensors are low cost, the possibility of obtaining a pure material, good manufacturability, the linear dependence of resistance R_t from temperature t . Static characteristic of copper RTD is described by the equation: $R_t = R_0(1 + \alpha t)$, where α - temperature coefficient, R_0 - RTD resistance at 0 °C. The disadvantage of copper is its intense oxidation, which limits the range of application of copper RTD with 200 °C temperature and requires enameling or

silicone isolation of sensor wire. The sensor consists of 0.1 mm in diameter insulated copper wire, which wound on a frame (Figure 19a). (Ivanova G.M. et al. 2005, 54.)

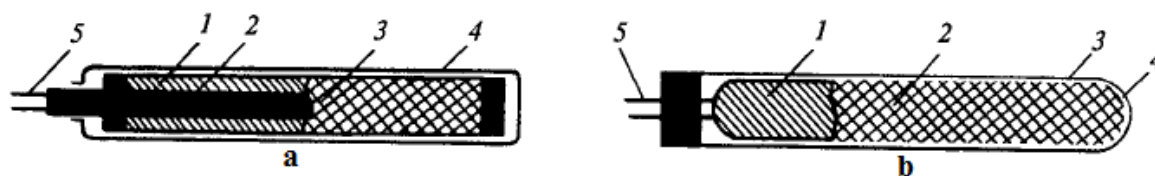


Figure 19. Copper resistance thermometers sensors. (Ivanova G.M. et al. 2005, 54.)

a – with frame winding; 1 – winding; 2 – frame; 3 – layer of varnish; 4 – protective shell; 5 – junctions; b – without frame winding; 1 – winding; 2 – fluoroplastic coating; 3 – protective shell; 4 – insulating powder; 5 – junctions

In this case, the inductive reactance of the sensor should be minimal. The sensor comprises a large number of turns of copper wire, and with normal winding it will have a higher inductance. As secondary devices have measuring circuits, which are supplied with alternating current, inductive reactance of one of the arms (sensor) will affect the balancing mode. To provide a non-inductive mode commonly bifilar winding is used - winding with a wire folded in half. The surface of the winding is covered with a layer of varnish. To the junctions of the wire copper terminals with diameter 1...1,5 mm are soldered. The sensor is placed inside a sealed metal protective shell covered with an insulating powder. Sensors also can be frameless (Figure 8b). They are made of a copper wire (diameter 0.08 mm) with non-inductive winding. The individual layers are bonded with varnish, and then the whole sensor wrapped with fluoroplastic coating. Sensor is placed in a thin-walled sealed metal shell that is filled with an insulating powder. The drawback of copper as a material for the resistance thermometer is also a small specific resistance, manufacturing of sensors thus requires a lot of wire, which increases the size of the sensor and deteriorates the dynamic properties of the RTD. Connecting RTD to the secondary instrument can be carried out with two-, three- or four-wire schemes. (Ivanova G.M. et al. 2005, 54-56.)

4.1.2 Thermoelectric temperature sensor

Thermoelectric temperature sensor, or thermocouple is also one of the most common technique of measuring temperature. Thermoelectric temperature measurement method is based on the thermoelectromotive forces (thermo-EMF) dependence on the thermocouple hot junction temperature. Thermo-EMF arises in circuit consisting of two dissimilar conductors (electrodes), if temperatures of junctions t and t_0 are not equal (if equal, then thermo-EMF is zero). EMF present in thermocouple circuit is the result of Seebeck and Thomson effects. The former relates to the EMF appearance in a junction point of two dissimilar conductors, and the magnitude of the EMF depends on the temperature of the junction. Thomson effect is associated with the occurrence of EMF in the uniform conductor with a temperature difference available between its terminals. (Gordov A.N. et al. 1992, 68.)

Thermo-EMF depends on the value of both temperatures t and t_0 , and it increases with the difference $(t - t_0)$. Therefore, thermo-EMF is conventionally denoted with $E(t, t_0)$ sign. It is obvious that the temperature can be measured using a thermocouple if the following requirements are met: the hot junction of a thermocouple is placed in a controlled environment and cold junction temperature is known, EMF of the thermocouple is measured and the calibration characteristic $E(t, t_0)$ of the thermocouple is known. (Gordov A.N. et al. 1992, 69.)

One of the properties of the thermocouple is explained with the third conductor theorem. The essence of it is that the inclusion of the third (any material) conductor in thermocouple circuit (Figure 20) does not cause distortion of thermo-EMF, if temperatures of the conductor's junctions are the same. (Gordov A.N. et al. 1992, 70.)

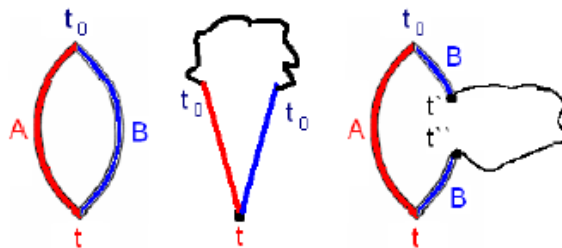


Figure 20. Third conductor theorem illustration. (Ivanova G.M. et al. 2005, 59.)

Any two dissimilar conductors may form a thermocouple, but not an every thermocouple can be used for practical temperature measurements. The materials for thermocouples must meet a number of requirements: heat resistance, chemical stability and reproducibility of materials (to ensure changeability of thermocouples). Thermo-EMF $E(t, t_0)$ of a thermocouple depends on the hot junction temperature t and cold junctions temperature t_0 . There is a general formula of $E(t, t_0)$ and t_0 dependency:

$$E(t, t_0) = E(t, 0) - E(t_0, 0). \quad (39)$$

Thus, if values t_0 and $E(t, t_0)$ are known, then using the nominal static characteristics (Figure 21) one can determine the value of t as follows:

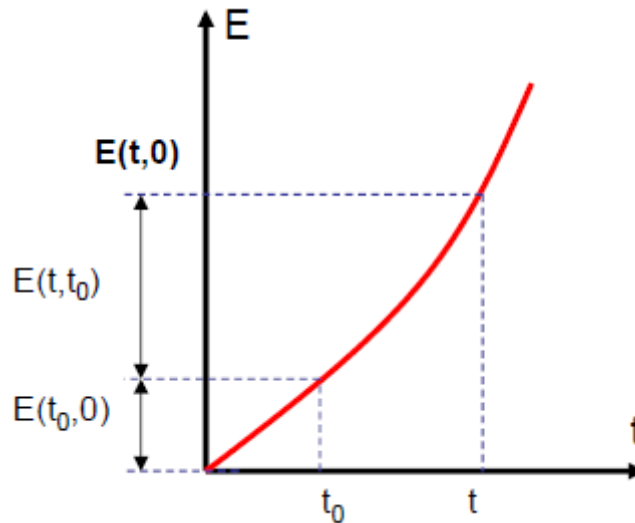


Figure 21. Nominal static characteristics example. (Gordov A.N. et al. 1992, 70.)

- Find $E(t_0, 0)$ value;
- Sum $E(t_0, 0)$ with measured $E(t, t_0)$ value;
- Using $E(t, 0)$ determine temperature t ; (Gordov A.N. et al. 1992, 70.)

In practice t_0 is varied ambient temperature, where thermocouple cold-junctions are located. So usually it is corrected with an automatic compensator. For measuring ambient temperature compensators comprise a sensor which temperature is equal to t_0 . In some cases, cold-junctions temperature of the thermocouple and temperature of this sensor in the compensator are very different. Then the thermocouple must be connected to the

compensator with special wires - thermocouple wires. Properties of these wires should be identical to thermocouple electrodes. This means that the calibration characteristics of materials of thermocouple wires must match the characteristics of the thermocouple electrodes in the range of possible temperature t_0 changes. A need of use these wires disappears when thermocouples have built-in head normalizing transducer, which correct cold-junctions temperatures of the thermocouple. The output signal is a unified signal or a digital signal. (Gordov A.N. et al. 1992, 71-72.)

Conditionally, thermocouples are divided into general purpose industrial thermocouples and special thermocouples. Sheeted thermocouple is a thermocouple with insulated electrodes placed in a protective sheet. The Figure 22 shows a design of one variety for general industrial use. The electrodes *1* are usually made of heavy gauge wire, providing negligible resistance, and sufficient mechanical strength. Hot junction *2* is usually done by welding. For thermal insulation of the electrodes quartz (up to 1000 °C) or porcelain tube (up to 1400 °C) are used. At higher temperatures metal oxides are used: aluminum, magnesium, beryllium etc. In Figure 22 tube marked *3* represents an insulator consisting of the rod with two longitudinal holes into which electrodes are passed through. Hot junction can be protected with ceramic tip *5*. Material of sheet *4* is normally stainless steel (900 °C), at high temperatures special alloys are applied. Sheet ends in the housing *7*, which contains sensor connection *8* with terminals *9*. These terminals are connected to the electrodes of the thermocouple through a sealed input *11* and to the thermocouple wires *10*. Inner cavity of the sheet may be sealed-up in the upper part *6*. On the outer surface of the sheet *2* a penetration gland can be installed to enable sensor installation in piping or vessels. Length of section *L* of varies and can be anything from 0.08 to 2.5 m. Diameter of the sheet can be from 5 to 25 mm. (Ivanova G.M. et al. 2005, 68-69.)

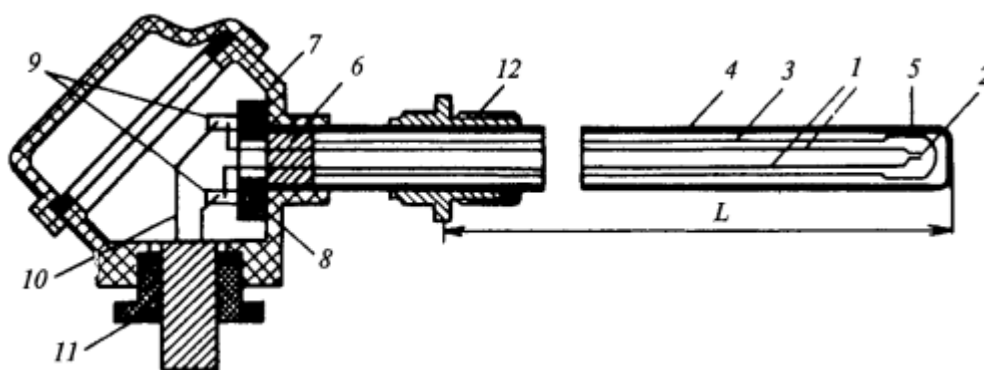


Figure 22. Design of the general purpose industrial thermoelectric sensor. (Ivanova G.M. et al. 2005, 69.)

Special thermocouples are designed to measure the temperature in the range -50 to $1000\text{ }^{\circ}\text{C}$ and are mainly used in the reactor thermometry. Thermocouples have an outer cable diameter of between 1 to 6 mm, a length of 10 to 50 m with 2 or 4 conductors. The design of the thermocouple with insulated hot junction is schematically shown in Figure 23. (Ivanova G.M. et al. 2005, 70.)

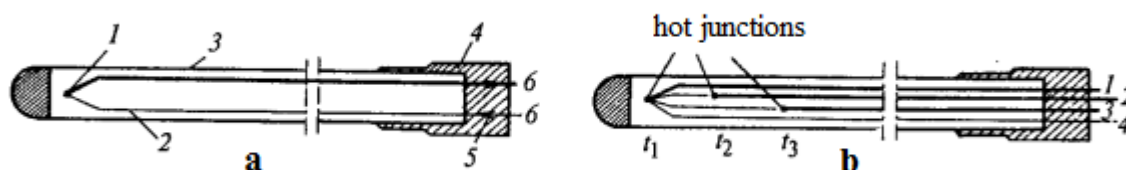


Figure 23. Design of the thermocouple of special application. (Ivanova G.M. et al. 2005, 70.)

a – one-point transducer, b – multipoint transducer

In sheeted transducers insulation of electrodes is done with compressed magnesium oxide. A significant drawback is its hygroscopicity, and in high humidity it swells, can break the shell and loses insulating properties. The shell material is a stainless steel. Thermocouple electrodes with a small diameter are very thin and have a large linear resistance. To increase the strength and reduce the resistance of the measuring circuit in the plug 4 they are thickened with conductor material. There are transducers with thinning or flat working tip. As an insulator aluminum oxide can be used. It has good insulating properties up to $1200\text{ }^{\circ}\text{C}$, radiation-resistant but like magnesium oxide, it is also hygroscopic although does not swell, when wet. Its drawback is the hardness of crystals, which does not provide dense

packing and consequently high isolation. For temperatures up to 2000 °C beryllium oxide can be used, which drawback is toxicity. (Lysikov B.V., Prozorov V.K. 1980, 43-44.)

Specific requirements for the shell materials of thermocouples in reactor measurements are minimal neutron absorption cross section, minimal induced activity, high radiation resistance, high corrosive resistance and manufacturability. Therefore iron with a high content of nickel is used. (Ivanova G.M. et al. 2005, 71.)

To measure the temperature at several points sheeted multipoint thermocouples can be used (Figure 23b). The advantages of such thermoelectric transducers are: the ability to measure temperature at several points in tight spaces due to the large length and small diameter with a small amount of metal introduced in a controlled environment. (Ivanova G.M. et al. 2005, 71.)

4.2 Pressure and pressure difference measurements

Monitoring of most processes in the nuclear industry is connected with measurements of pressure or differential pressure of gaseous and liquid media. Pressure is a large concept that characterizes normally distributed force exerted by a body on the surface unit of another one. If it is liquid or gas, the pressure, describing the internal energy of the media, is one of the state variables. In measurements one can distinguish absolute, gage and vacuum pressure. Absolute pressure p_a is a total pressure, which is equal to the sum of atmospheric pressure p_{at} and gage pressure p_g :

$$p_a = p_g + p_{at}. \quad (40)$$

The concept of the vacuum pressure is introduced in pressure measurements below atmospheric pressure: $p_v = p_{at} - p_a$.

Electrical pressure sensors have found widespread application in nuclear power plants: piezoelectric converters, piezoresistive strain gauges, capacitive pressure sensors. (Gonek N.F. 1979, 15.)

4.2.1 Piezoelectric converters

The principle of operation of this type of sensors is based on the piezoelectric effect, which consists of the appearance of electrical charges on the surface of the compressed quartz plate. This plate is cut out in perpendicular direction to the electric axis of quartz crystals. Scheme of a piezoelectric converter is shown in Figure 24. Measured pressure via the membrane 1 is converted into a force compressing quartz plate 2. The electric charge appearing on the metallized planes 3 by the force F from the membrane is determined by the expression:

$$Q = kF = kSp, \quad (41)$$

where p – pressure acting on the metallic membrane 1 with an effective area S , k – piezoelectric constant, C/N. (Ivanova G.M. et al. 2005, 199.)

The voltage in the input of the amplifier connected to the output of the piezoelectric transducer is determined by the total capacity of the circuit C : $u = Q/C$.

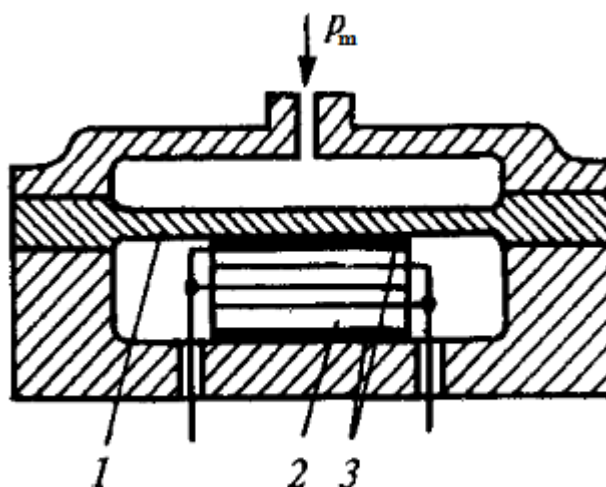


Figure 24. Scheme piezoelectric converter. (Ivanova G.M. et al. 2005, 199.)

Quartz, in contrast with other ferroelectrics having piezoelectric effect, is mechanically strong and has a high rigidity which excludes the influence of the elastic characteristics of the membrane *1* on the transmission coefficient of the piezoelectric transducer. The free frequency of the converter reaches tens of kilohertz, so that they are used in testing, characterized by high-frequency changes of the pressure. The piezoelectric constant of quartz (about $2 \cdot 10^{-12}$ C/N) is stable and weakly dependent on temperature, which allows the use of piezoelectric transducers in measuring pressure of high-temperature media. Because of the charge leakage piezoelectric transducers are not used to measure static pressure. In order to increase the sensitivity several quartz plates are connected in parallel. The upper limit of the measuring pressure of these devices is 100 MPa. (Ivanova G.M. et al. 2005, 200.)

4.2.2 Piezoresistive strain gauge

Piezoresistive strain gauges approach the piezoelectric gauges in frequency characteristics. Their sensors are membranes that contain wire, foil or semiconductor resistors which resistance varies with membrane deformation caused by pressure. Wire resistance strain

gauges are easier to manufacture, but their sensitivity factor, defined as the ratio of the relative change in the resistance to deformation, is an order of magnitude less than what semiconductor resistance strain gauges have. (Ivanova G.M. et al. 2005, 200.)

Currently available pressure transducers are based on silicon on sapphire structure. In these devices sapphire membrane with deposited silicon resistors is used for converting pressure impact power into an electrical signal. The design of a piezoresistive strain gauge is shown in Figure 25a. A sensor is a piezo converter 1 with a two-layer membrane. The measured pressure acts on titanium membrane which is on top of a sapphire membrane with strain gauges is soldered to it. The elements of the measurement circuit and the amplifier are in the block 2. (Ivanova G.M. et al. 2005, 201.)

There are 2 types of piezoresistive strain gauges: pressure type (Figure 25a) and force type (Figure 25b). In pressure type of converters, measured pressure acts directly on the membrane. At 0.4 MPa and a higher pressure, forces on membrane with diameter 6 ... 8 mm are sufficient to deform it. So, in force type converters lower metal membrane 4 has a lever 3, to which force is exerted and developed by the membrane unit under pressure. (Ivanova G.M. et al. 2005, 201.)

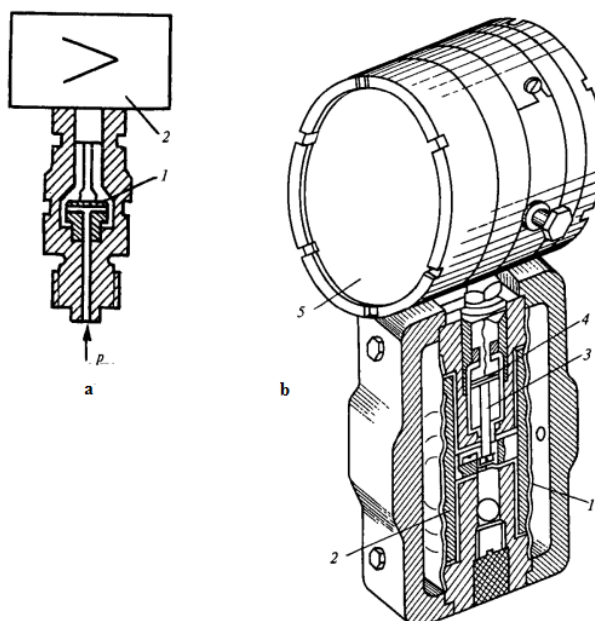


Figure 25 a – pressure-type of piezoresistive strain gauge;
b – force-type of piezoresistive strain gauge. (Ivanova G.M. et al. 2005, 201.)

The rigidity of the membrane unit is greatly determined by the rigidity of the membrane-lever transducer (force-type). Offset of centers of membranes leads to bending of the lever 3 and of the sapphire diaphragm with strain gauges 4. The amplifier circuit elements are located in the measuring block 5. (Ivanova G.M. et al. 2005, 202.)

Principle scheme of the resistors location on the surface of the sapphire membrane is shown in Fig. 26a. When there is a deformation of the membrane in accordance with diagram shown in Figure 26b, shear stresses σ_t have constant sign, whereas radial σ_r change it. In this regard, strain gages radially disposed near the edge of the membrane resistance decreases when pressure increases, but resistance of strain gages placed tangentially increases. Choosing a location point of strain gages provides sensitivity increasing of the measuring system. (Ivanova G.M. et al. 2005, 202.)

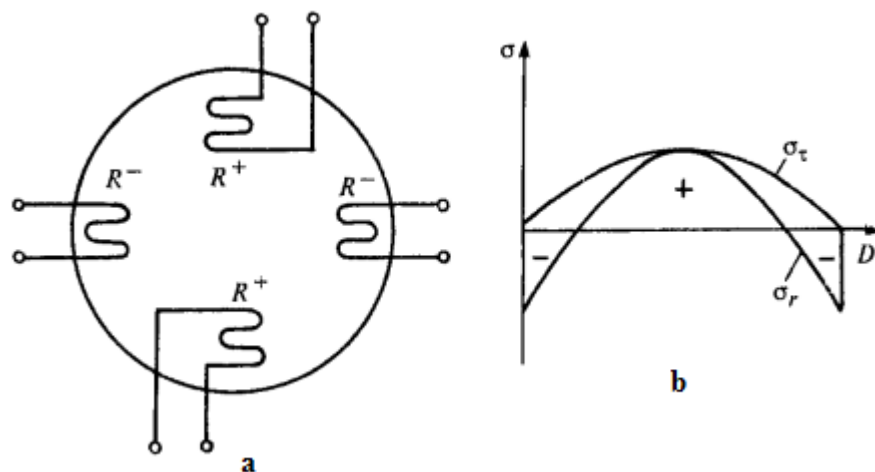


Figure 26. a - the arrangement of strain gages on the membrane;
b – stress diagram. (Ivanova G.M. et al. 2005, 202.)

Simplified diagram of the analog converter is shown in the Figure 27. Electronic amplifier is a device with a negative feedback. Strain gages $R_1 - R_4$ form a balanced bridge witch imbalance signal depends on the measured pressure. If the bridge arms are symmetrical, i.e. $R_1 = R_3 = R_0(1 + kp)$, $R_2 = R_4 = R_0(1 - kp)$, then $R_1 + R_2 = R_3 + R_4$ и $I_1 + I_2 = I_b/2$.

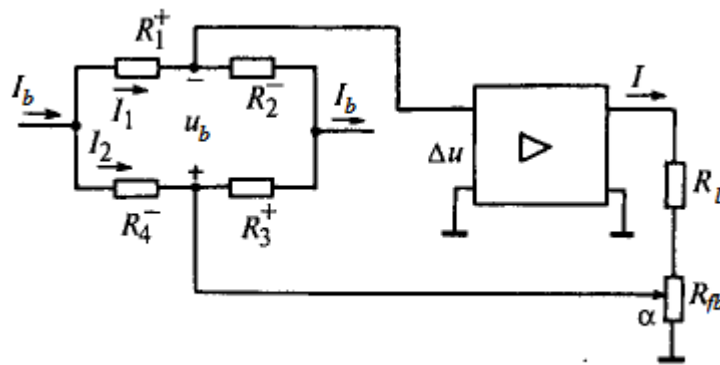


Figure 27. Simplified diagram of the analog converter. (Ivanova G.M. et al. 2005, 203.)

With infinite input the impedance of the amplifier $u_b = \frac{R_0(1+kp)I_b}{2} - \frac{R_0(1-kp)I_b}{2} = kR_0I_bp$. Supply current of the bridge is stabilized, constancy conversion factor is provided by the introduction of a negative feedback, withdrawn from the share α of feedback resistor R_{fb} . This resistance is in series connection with the load resistance R_l . With an infinitely large gain amplifier $\Delta u = u_b - I\alpha R_{fb} \cong 0$, whence $I = kR_0I_b/(\alpha R_{fb})p$. Changing α and R_{fb} , adjust the measuring range. (Ivanova G.M. et al. 2005, 203.)

A disadvantage of this type of transducers is a large temperature coefficient around 0,1 %/°C. Therefore, there is temperature compensation in all converters, which is based on the temperature characteristics of each individual unit. The main advantage of pressure measurement with piezoresistive strain gauges is the use of small deformations of the sensors, which increases their reliability and stability characteristics, and provides vibration resistance. (Ivanova G.M. et al. 2005, 207.)

4.2.3 Capacitive pressure sensors

Intelligent capacitive pressure sensors have high metrological characteristics. Scheme of microprocessor of Fischer-Rosemount pressure transducer is shown in Figure 28. The measured pressure or pressure differential affects the isolation diaphragms 1, between which a cavity filled with a neutral liquid, sensitive membrane 2 is located. This membrane is a moving plate of the differential capacitor which fixed plates are the chamber walls 3

and 4. These converters have the current signal in the output 4...20 mA, the voltage signal 0.8...3.2 V and 1...5 V, HART-protocol. Differential pressure gauge can have linear and quadratic conversion; the device can have a digital indicator. (Ivanova G.M. et al. 2005, 207.)

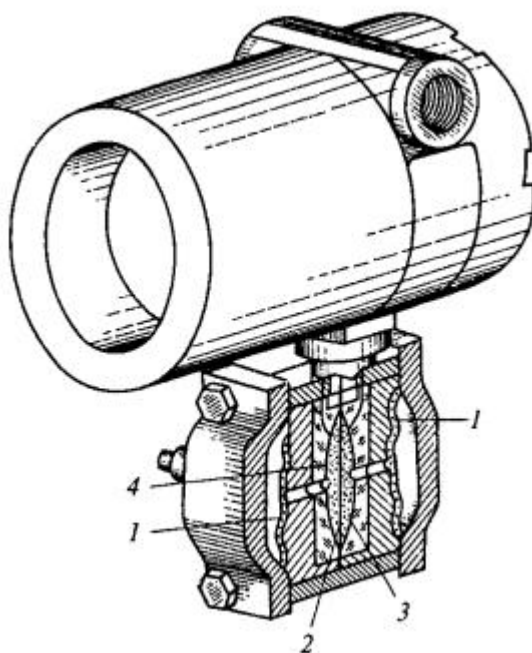


Figure 28. Pressure gauge with capacitive transducer. (Ivanova G.M. et al. 2005, 207.)

Transducers measure the absolute pressure of from 6.22 to 6895 kPa, a gage pressure from 0.49 to 4136 kPa, a pressure difference of 0.49 to 4136 kPa, a hydrostatic pressure of 6.2 to 689.5 kPa. Error limit is $\pm 0,1$; $\pm 0,2$; $\pm 0,25$ %. (Ivanova G.M. et al. 2005, 208.)

4.3 Level measurements

Level measurements of liquids are important in process automation, particularly if it is associated with safe operation of the equipment, such as nuclear power plants. Level gauges are used either for monitoring the deviation from the nominal level in which case they have a double-sided scale, or to determine the amount of substance, in which case they have a single sided scale. Level alarms form a large group in which the output signal occurs when the level reaches the upper or lower limit values. Depending on the measurement conditions and the nature of the controlled medium different measurement methods are used. If the remote transmission of readings is necessary, hydrostatic, buoy, float, capacitive, inductive, radioisotope, wave, acoustic or thermoconductometric gauges are applied. The most widespread level measurement methods in nuclear power plants are hydrostatic and float methods, buoyancy and capacitive methods are less used, and other techniques are limited in their application. (Bobrovnikov G.N. Katkov A.G. 1977, 21.)

4.3.1 D/p level transmitters

Level gauges measure liquid level H with constant density ρ and of the hydrostatic pressure p produced by the fluid, and column,

$$p = H\rho g. \quad (42)$$

Level measurement can be carried out in tanks, which are both under atmospheric, or under a pressure different from atmospheric.

The simplest scheme of the level measurement in the tank under pressure is shown in Figure 29. Reference vessel 1 is connected to the vapor part and the vessel and the pipe 2 are not covered by thermal insulation which provides a constant level in the reference vessel due to drain of an excess condensate into the tank. The tube 3 is connected directly to the water part of the tank. The value for the pressure difference Δp measured with differential pressure gauge 4 can be easily obtained with the pressure p_1 and p_2 generated in the tap 1 and tap 2 of differential pressure cells:

$$p_1 = (H + H_0)\rho_w g + p_r, \quad (43)$$

Where ρ_w – density of water in reference vessel and tap 1; p_r – pressure in reservoir.
(Ivanova G.M. et al. 2005, 220-224.)

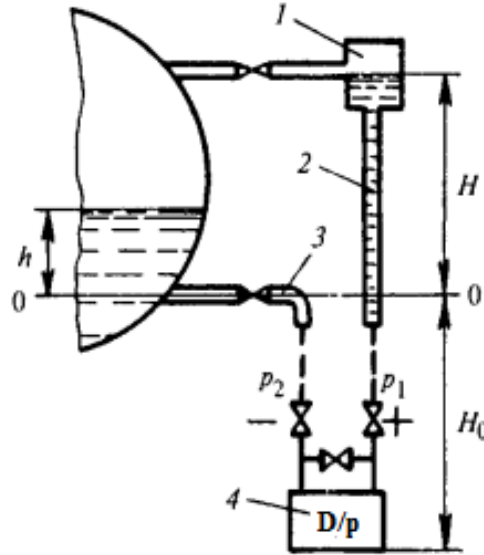


Figure 29. Scheme of the level gauge with single-chambered reference vessel. (Ivanova G.M. et al. 2005, 223.)

Pressure p_2 represents p_r plus the amount of hydrostatic pressure of the liquid column h in the tank, having a density ρ' , the liquid column H_0 in the impulse tap 3 with density ρ_w and steam column $(H - h)$ with density ρ'' :

$$p_2 = H_0 \rho_w g + h \rho' g + (H - h) \rho'' g + p_r. \quad (44)$$

Thus, the pressure difference Δp , acting on the differential pressure gauge, is given by:

$$\Delta p = p_1 - p_2 = (H(\rho_w - \rho'') - h(\rho' - \rho''))g. \quad (45)$$

It is easy to notice that the level gauge readings depend not only on the current value, but also on the density of water ρ' and of steam ρ'' , which in turn depend on the temperature and pressure of the fluid in the reservoir. In addition, the measurement result is influenced by changes of water density in the reference line ρ_w , as this changes the hydrostatic pressure of the column with height H in the tap 2, while p_1 pressure should remain constant. This may occur when the ambient temperature or the temperature of the medium in the tank changes. (Ivanova G.M. et al. 2005, 224.)

Reducing the impact of ρ_w changes on gauge readings can be achieved using a compound surge tank (Figure 30). The surface of the vessel 1 is covered with thermal insulation to make the density of water in it and density of water in the inner tube 2 equal to the density of water in the tank. For this scheme an expression of differential pressure acting on the differential pressure gauge 3 is of the form

$$\Delta p = (H - h)(\rho' - \rho'')g. \quad (46)$$

Where ρ' and ρ'' - the densities of water and steam in the reservoir. Thus, when using this scheme gauge readings depend on the difference between the density of water and vapor $\rho' - \rho''$, which is determined by the operation of the unit. (Ivanova G.M. et al. 2005, 224.)

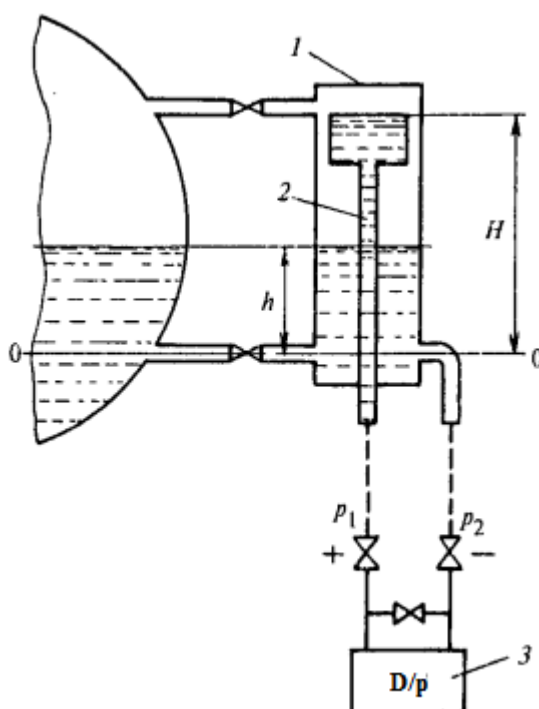


Figure 30. Scheme of level gauge with compound a serge tank. (Ivanova G.M. et al. 2005, 225.)

Differential pressure method of measuring level has a number of advantages: mechanical strength, ease of installation and reliability. But it also has a major drawback: the sensor of D/p transmitter is in direct contact with a controlled environment. When measuring the level of aggressive media it is necessary either to use special materials for sensors or apply special connection schemes, which prevent the interaction between the active media and manometer, such as inclusion in the impulse taps separating devices, blowdown of impulse taps with clean water, etc. (Bobrovnikov G.N. Katkov A.G. 1977, 41.)

4.3.2 Float level indicator

Float level indicator is based on the position measurement of the float, partially submerged in the liquid. Submersion of the float (draft) at a constant fluid density does not depend on a controlled level. The float is moved vertically together with the liquid level, and thus knowing its position a level value can be determined. In the static mode following forces act on the float: the force of gravity G , and buoyant forces of the liquid and gaseous medium. When the float moves resistance force appears in moving elements of the device. If we neglect the resistance force of kinematical connections and buoyancy force of the gas phase, the forces acting on the float are connected by the equation $G = V_1 \rho_1 g$, where, V_1 – volume of a submersed part of the float and ρ_1 – density of liquid. The volume of the submerged part of the float V_1 and, thus, draft of the float, is a parameter that determines the additional error caused by the density change of the liquid. To reduce this error it is needed to reduce the draft of the float, which can be achieved either by increasing the cross sectional area or lighting of the float. (Ivanova G.M. et al. 2005, 231.)

At high temperatures and pressures magnetic float level indicators are used (Figure 31). On the guide tube 7 under the influence of level changes the float 6 moves with the permanent magnet 5. Inside the tube 7 over its entire length reed relays 8 are situated, which are activated by the magnetic field of the float. Retaining ring 4 limits the movement of the float upwards and the umbrella 3 protects it from condensation that may form on the inner walls of the tank. When determining the weight to account for density changes of the liquid there is a temperature measurement in the device. These transducers can have an output as a change in resistance value, a signal of 4 ... 20 mA or digital. (Ivanova G.M. et al. 2005, 232.)

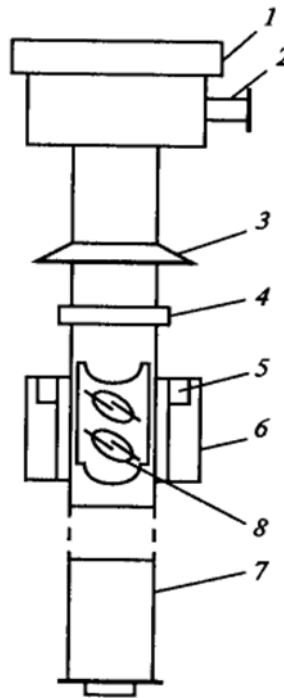


Figure 31. Scheme of magnetic float level indicator.

1 – frame; 2 – cable termination; 3 – umbrella; 4 – retaining ring;
5 – permanent magnet; 6 – float; 7 – guide tube; 8 – reed relays
(Ivanova G.M. et al. 2005, 232.)

4.3.3 Buoyancy level transmitter

Buoyancy level transmitters are based on Archimedes' principle: dependency of the buoyant force acting on the buoy on the liquid level. A sensor of such gauges is a massive body (e.g. cylinder) - vertically suspended buoy inside the vessel and partially submerged in the controlled liquid (Figure 32). Buoy is fixed to the elastic spring which has a stiffness c and it acts on the buoy with a certain torque. By increasing the level from the zero level to H , we increase the buoyancy force that causes the buoy rise to x , and its draft also rises, i.e. $x < h$. This changes the force which acts on the buoy by spring, and the change is equal to a change of a buoyancy force caused by the increase of buoy's draft ($h - x$):

$$xc = (h - x)\rho_l gF - (h - x)\rho_g gF, \quad (47)$$

where c – spring stiffness, ρ_l, ρ_g – densities of liquid and gas; F – cross-sectional area of the buoy. (Ivanova G.M. et al. 2005, 232-233.)

It is easy to obtain an expression for the static characteristics of a buoy:

$$x = \frac{h}{1 + c(\rho_1 - \rho_g)gF}. \quad (48)$$

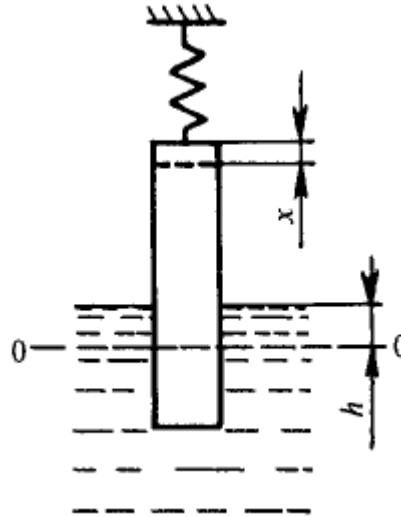


Figure 32. Calculation model of a buoyancy level transmitter. (Ivanova G.M. et al. 2005, 233.)

Thus, static characteristic of the buoyancy level transmitter is linear, wherein its sensitivity can be changed by increasing of F or decreasing spring stiffness c .

A scheme of the buoyancy level transmitter is shown in Figure 33.

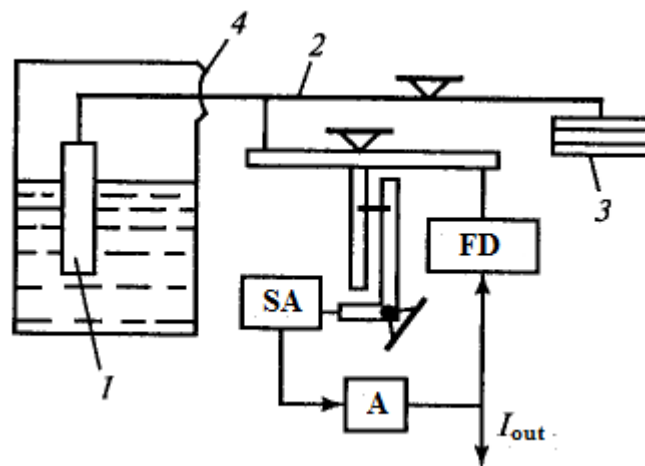


Figure 33. Scheme of the buoyancy level transmitter. (Ivanova G.M. et al. 2005, 234.)

The buoy is suspended on one end of the lever 2, on the other end of which is a weight 3, balancing the buoy weight at zero level. Separation membrane 4 serves to seal the tank. When you change the level, the tension with which the buoy acts on the lever also varies.

Imbalance of forces leads to a shift of the lever and core of a differential transformer converter, which acts as a synchronization annunciator SA. Its output signal is fed to an amplifier A, which output signal I_{out} is fed to the input of the device and to the feedback device FD. The latter represents the electric power converter, which creates the force, eliminating the imbalance of forces. (Ivanova G.M. et al. 2005, 234.)

Buoyancy level transmitters are used to measure the level of non-viscous and viscous, non-sedimentary, non-crystallizable media under pressure - (4 ... 16) MPa and temperatures from -200 to 200 ° C, the density of the medium is (600 ... 2500) kg/m³. (Ivanova G.M. et al. 2005, 234.)

4.3.4 Capacitive level indicators

Capacitive level indicators are based on the dependence of the electrical capacitance of the condenser transducer, formed by one or more rods, cylinders or plates, partially inserted into the liquid. (Ivanova G.M. et al. 2005, 235.)

The design of capacitor transducers is different for conductive and non-conductive fluids. Conductive liquids are liquids having an electrical resistivity $\rho < 10^6$ Ohm·m and a dielectric constant $\varepsilon \geq 7$. The difference in transducers is that one of the electrodes of level indicators for conductive liquids is covered by an insulating layer, and electrodes of the transducers for non-conductive liquids are not isolated. Electrodes can have a form of flat plates or rods. The metal wall of the vessel can be used as the electrode. Frequently used cylindrical electrodes have a good process ability compared with other forms of electrodes, have a better noise immunity and provide greater rigidity. (Ivanova G.M. et al. 2005, 235.)

A capacitive level indicator for non-conductive fluids, comprising of two coaxial electrodes 1 and 2 placed in the reservoir 3, wherein the level measurement is conducted, is shown in Figure 34a.

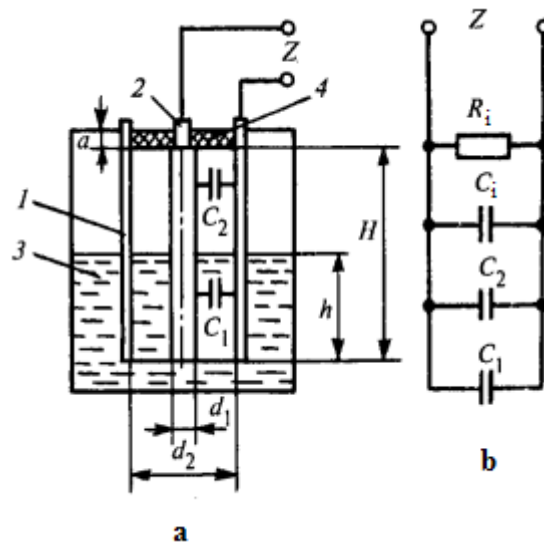


Figure 34. a - capacitance level indicator for non-conductive fluids
b – electrical scheme of level indicator. (Ivanova G.M. et al. 2005, 235.)

The mutual bracing of electrodes is fixed with bushing insulator 4. Electrodes form a cylindrical capacitor, in which part of an interelectrode space with a height H is filled with a fluid and the rest of the height ($H-h$) is filled with its vapors. In general, the capacitance of the cylindrical capacitor is defined with expression

$$C = \frac{2\pi\epsilon\epsilon_0 H}{\ln\left(\frac{d_2}{d_1}\right)}, \quad (49)$$

where $\epsilon_0 = 8,85 \cdot 10^{-12}$ F/m – dielectric constant, ϵ - relative dielectric constant that fills the interelectrode space, H – height of electrodes, d_1, d_2 - inner and outer electrode diameters. (Ivanova G.M. et al. 2005, 236.)

On the basis of (36) can be written an expression for the capacitance C_1 of the transducer which is in a liquid, and the capacitance C_2 of the transducer in a gas space:

$$C_1 = \frac{2\pi\epsilon_1\epsilon_0 h}{\ln\left(\frac{d_2}{d_1}\right)}; \quad C_2 = \frac{2\pi\epsilon_g\epsilon_0 (H-h)}{\ln\left(\frac{d_2}{d_1}\right)}, \quad (50)$$

where ϵ_1 and ϵ_g - relative dielectric constants of liquid and gas.

The total output resistance of the transducer Z , beside those C_1 and C_2 , is also defined by the capacity C_i of the bushing insulator and its active resistance R_i as well as capacitance and conductance of the connecting cable. (Ivanova G.M. et al. 2005, 236.)

Thus, the electrical scheme of the transducer is as shown in the Figure 23b. The total capacity of the device

$$C = C_1 + C_2 + C_i. \quad (51)$$

Capacity C_i does not depend on h , moreover, for gases $\varepsilon_g \approx 1$ therefore

$$C = C_i + \frac{2\pi\varepsilon_0}{\ln\left(\frac{d_2}{d_1}\right)} H[1 + (\varepsilon_l - 1)h/H]. \quad (52)$$

Thus, when $\varepsilon_l = \text{const}$, capacity C is uniquely dependent on the measured level h . Under real conditions ε_l may vary depending on temperature, fluid composition, etc. (Ivanova G.M. et al. 2005, 236.)

To reduce the impact of ε_l on the level indicator readings compensation capacitor is commonly used (Figure 24). Here, 1 and 2 are electrodes of the transducer, which capacitance depends on the measured level and ε_l value. The lower part of the electrode 1 and additional electrode 3 form a compensation capacitor which is always immersed in the liquid, and therefore, its capacity depends only on ε_l . A capacitance of the compensation capacitor is used in the electrical scheme as a correction signal. (Ivanova G.M. et al. 2005, 236-237.)

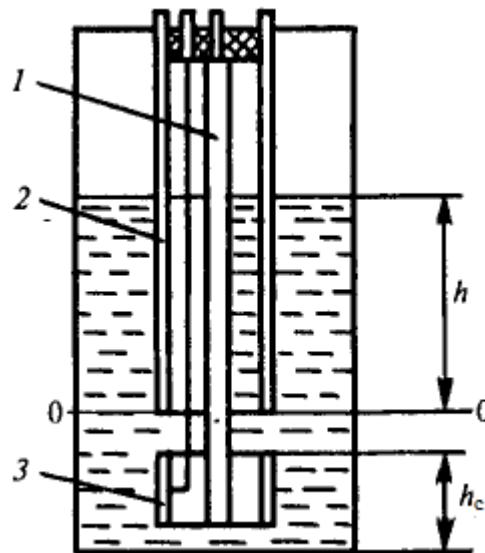


Figure 35. Scheme of the transducer with the compensation capacitor. (Ivanova G.M. et al. 2005, 237.)

The disadvantage of such a compensation scheme is an increase of non-measured level in comparison with the scheme in Figure 34 caused by the height h_c of compensation capacitor electrodes. The negative impact on the operation of capacitance level indicators

is associated with a resistance R_i of bushing insulator and a controlled fluid resistance in the interelectrode space, which forms the total resistance of the transducer. To reduce the influence of the resistance in transducer circuit a phase detector is connected to it. In capacitor transducers for conductive liquids one electrode is isolated. If the tank is metal, its walls can be used as the second electrode. (Ivanova G.M. et al. 2005, 237.)

If the tank is non-metallic, then an insulated metal rod is installed in the liquid, acting as a second electrode. Figure 25a shows a transducer drawing a rod 1 covered with an insulation layer 2 and immersed in a metal tank 3 . If we neglect the permittivity of electrode insulation, then electrical scheme may be represented as shown in Figure 36b. In accordance with this scheme, the total capacity of the device is given by

$$C = C_i + \frac{C_1 C_2}{C_1 + C_2}. \quad (53)$$

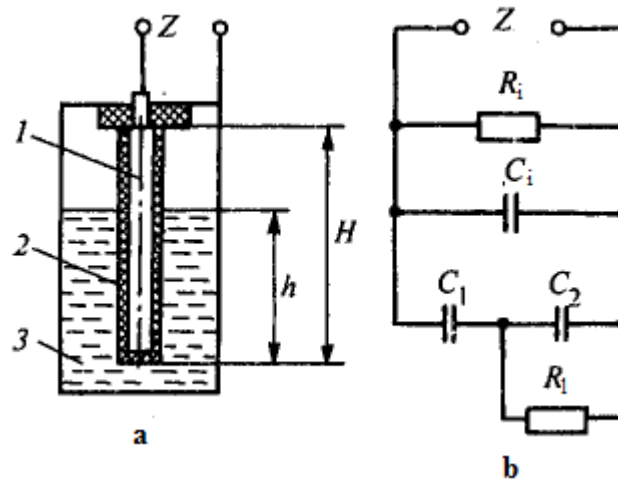


Figure 36. Scheme of the capacitance level indicator for conductive liquids. (Ivanova G.M. et al. 2005, 237.)

There are different schemes used for measuring the electrical capacity of capacitive level indicators. The simplest are the bridge circuits. The bridge consists of two secondary windings I and II of the transformer Tr (powered by generator G), transducer capacitance C and a trimming capacitor C_{tc} . The bridge is balanced when zero liquid level and the signal at the input and output of the amplifier is zero. By increasing the level capacity C rises, leading to growing imbalance of the bridge and increasing of the voltage at the input of the amplifier. In the amplifier this signal is amplified, converted to a standardized and measured secondary instrument SI. (Ivanova G.M. et al. 2005, 238-239.)

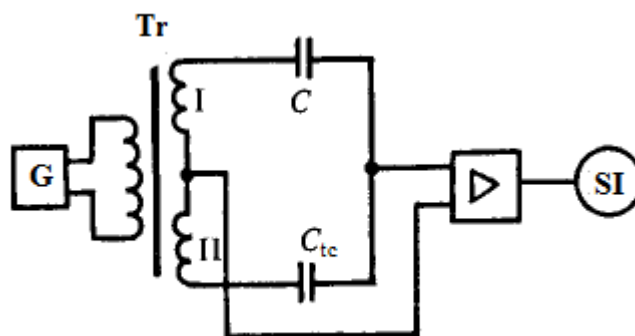


Figure 37. Principle scheme of the capacitance level indicator. (Ivanova G.M. et al. 2005, 239.)

Capacitive level indicators are wide applied as signaling indicators because of their low cost, ease of maintenance, ease of installation to the tank, the lack of moving parts and the possibility of using under a wide temperature and pressure range. Another big advantage is the insensitivity to strong magnetic fields. The disadvantages: they are unsuitable for the measurement of viscous, film-forming, crystallizing liquids and liquid containing impurities. Also problematic are precipitation and having high sensitivity to changes in the electrical properties of the liquid or the change in capacitance of the cable connecting the sensor to a measuring transmitter. (Ivanova G.M. et al. 2005, 240.)

4.4 Flow rate measurements

For measurements dealing with flow rates the most important initial concepts are volumetric and mass flow rate. Flow rate is an amount of the substance flowing through the cross section of a pipe per unit time. Accordingly, the measurement can be carried for mass flow rate G_m (units kg/s, kg/h, t/h) or volumetric flow rate G_v (m³/s, l/s, m³/h). The mass flow rate provide more complete information about the amount or flow of a substance than volume flow, as the volume depends on the pressure and temperature. (Kremlevskiy P.P. 1989, 6-8.)

When measuring flow rate, in most cases a working element is introduced into the medium, resulting a pressure loss. There are a variety of methods of flow rate measurements and flowmeter designs. In nuclear power plant the most widely used types of flowmeters are variable-pressure drop over throttle device, constant pressure difference, tachometric and electromagnetic flowmeters.

4.4.1 Variable-pressure drop method

This method of flow rate measurement is based on the dependence of the pressure drop over a fixed throttle device installed in the pipe and the flow of the medium. Generated differential pressure in throttle device is measured with differential pressure gauge. (Kremlevskiy P.P. 1989, 10.)

The measuring principle is that during the passing of the flow through the throat of orifice the flow rate increases compared to the rate before the throttle. Increasing speed and consequently increasing of kinetic energy causes a reduction of the potential energy and the static pressure. (Kremlevskiy P.P. 1989, 10.)

Flow rate can be determined by a known calibration curve $G = f(\Delta p)$ and by measuring the pressure difference Δp over throttle device by differential pressure gauge. This requires the fulfillment of certain requirements: the nature of the flow before and after the throttle device should be turbulent and stationary, flow must completely fill the cross section of the

pipeline, a phase state of flow should not change before and after the throttle device, inside the pipe before and after the throttle device sediments and other contaminants should not be formed, on the surfaces of the throttle device deposits changing its geometry should not be formed. (Kremlevskiy P.P. 1989, 10-12)

Multiple types of the throttle devices are used to measure the flow rate of liquids, gases and steam: orifice plates, nozzles and Venturi nozzles. An orifice plate (Figure 38a) is a thin disk with circular hole which axis is located along the pipe axis. Inlet (front) part of the hole has a cylindrical shape and then it merges into a conical extension. The front edge of the hole should be sharp without chamfers. Operating Reynolds number (Re) is dependent on the relative diameters of the throttle plate and it ranges from 10^5 to 10^8 . (Ivanova G.M. et al. 2005, 263.)

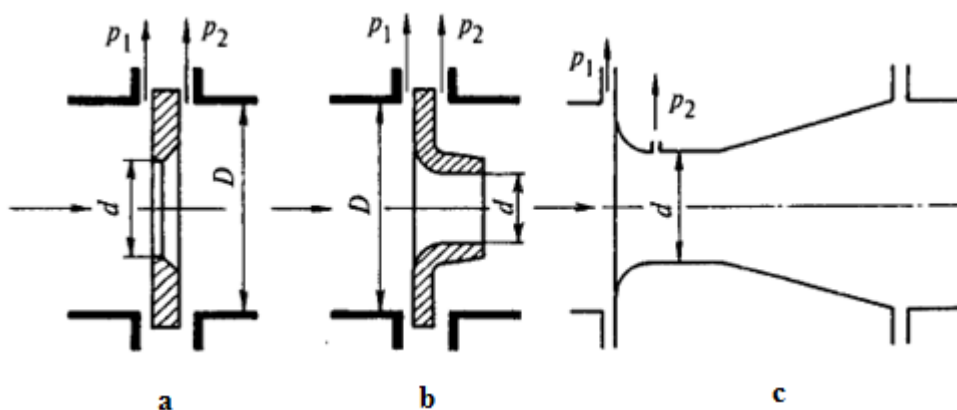


Figure 38. a – orifice plate, b – nozzle, c – Venturi nozzle. (Ivanova G.M. et al. 2005, 263.)

The *nozzle* (Figure 38b) has the profiled inlet part, which merges into the cylindrical section with diameter d . The butt end of the nozzle includes a cylindrical neck with a diameter greater than d to protect the discharge edge of the cylindrical part of the nozzle from damage. When measuring the flow rate the nozzle is installed in pipelines with diameter at least 50 mm, and the Re number should be $2 \cdot 10^4 \dots 10^7$. (Ivanova G.M. et al. 2005, 263-264.)

Venturi nozzle (Figure 38c) comprises an inlet part with the nozzle profile, merging into the cylindrical section and an outlet cone. The minimum diameter of the pipe for the standard Venturi nozzle is 65 mm. They are used in the range of Re numbers from $1,5 \cdot 10^5$ to $2 \cdot 10^6$. (Ivanova G.M. et al. 2005, 264.)

Calculation of the mass flow rate for incompressible fluids is conducted with the expression

$$G_m = CEf\sqrt{2\rho\Delta p}, \quad (54)$$

where $E = \frac{1}{(1-\beta^4)^{0.5}}$ is called velocity factor, f – minimum cross section area of the throttle device $\beta = d/D$ – relative diameter; C – discharge coefficient, which takes in account vortex of the flow in the inlet and outlet of throttle device and ρ – density of incompressible liquid. (Ivanova G.M. et al. 2005, 265.)

This formula is valid only for incompressible fluids. When measuring the flow rate of gas, vapor, air, their density decreases after the throttle device. To compensate this effect factor ε is used. To determine the mass flow rate of compressible fluids it is necessary to use the following formula:

$$G_m = CE\varepsilon f\sqrt{2\rho\Delta p}. \quad (55)$$

The values of C and ε are defined as a result of experimental studies conducted on pipes with a smooth inner surface and with flow velocity distribution over the cross section of the pipeline, which corresponds to a steady turbulent flow regime. (Ivanova G.M. et al. 2005, 265.)

Between a flow rate and pressure difference in the throttle device there is a quadratic dependence. The calibration of the differential pressure gauges must be done in square root settings in order to get the flow rate in engineering units from the transmitter. (Kremlevskiy P.P. 1989, 16.)

The need of taking the square root is one of the drawbacks of the method of measuring the differential pressure because it causes the narrowing of the measurement range. The suitable range is approximately 30 ... 100 % of the maximum flow rate. This means that the use of the flowmeter in the range of 0 ... 30% is not recommended, because there is no guarantee of adequate accuracy of the measurement. Another drawback is a pressure loss that occurs when throttle device is introduced inside the pipe. Under the same conditions,

the orifice plate has the largest, and Venturi tube the smallest loss. (Kremlevskiy P.P. 1989, 16.)

4.4.2 Velocity flowmeters

In velocity flowmeters movement of the working body is proportional to the volumetric flow rate of the medium. In most of cases, a working body rotates under the action of the flow. Flowmeters are classified into vane, turbine, ball-type, chambered, annular etc. types. (Kremlevskiy P.P. 1989, 612.)

Velocity flowmeters measure a volumetric flow rate, so to measure the mass flow rate they must be equipped with a temperature and pressure sensors, or densitometers and computing devices. (Kremlevskiy P.P. 1989, 612.)

Velocity flowmeters have following advantages: a wide dynamic range; high precision obtained by individual calibration of the device and ease of obtaining and taking readings. The disadvantages are significant pressure loss, demands to installation configuration, bearing runout because of the presence of contaminants in water and gas and restrictions on the diameter of the pipeline. (Kremlevskiy P.P. 1989, 613.)

Vane and turbine flow meters are used to measure a flow rate of various liquids except very viscous and contaminated, because the lubricity of the medium is important. Turbine flowmeters are seldom used to measure the flow rate of gas. This is due to the fact that the low density of the gas is insufficient to generate high torque except at high flow rates, which reduces the measuring range of the flowmeter, and increases the sensitivity threshold. Additionally, a bearing runout is more frequent in the gaseous medium. (Kremlevskiy P.P. 1989, 613.)

Vane flowmeters are applied on pipelines with a diameter from 15 to 40 mm, and from 50 to 250 mm turbine flowmeters are used. Figure 39 shows a turbine flowmeter. Transducer housing 1 is a tube with two flanges for attaching it to the pipeline. Straightening vanes 2 and 3 are mounted within the housing and are connected to the axis, on which the impeller

4 is situated. Rotation rate of the turbine, which is proportional to the volumetric flow rate, is converted into the pulse output signal by converter 5. The pulse signal is converted into an analog output signal. (Ivanova G.M. et al. 2005, 298-299.)

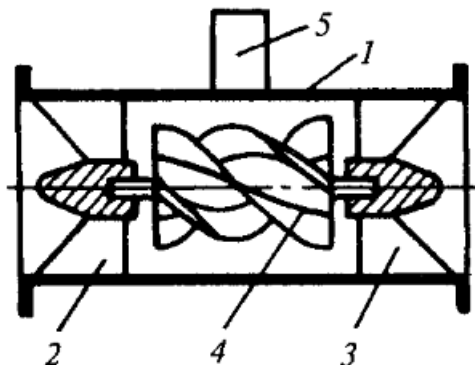


Figure 39. Turbine flowmeter scheme. (Ivanova G.M. et al. 2005, 299.)

For small loads on the turbine its rotation rate ω is proportional to the volumetric flow rate G_0 . However, this dependence is affected by the viscosity ν and the density ρ of the medium, a resistance moment M_r because of the friction in bearings and device reaction rate, the design parameters of the turbine. If viscosity increases and Reynolds number Re decreases, conversion coefficient ω/G_0 of the turbine flowmeter decreases. Turbine flowmeter readings dependence of the medium viscosity is a major disadvantage for this type of flowmeter. The resistance moment M_r effect is strongest when measured flow rates are small because the torque is reduced more than M_r . This fact limits the measurement range and causes a large measurement error in the initial part of the range. (Ivanova G.M. et al. 2005, 300.)

For non-contact measurement of rotation rate of the turbine its blades are made of ferromagnetic material or an impeller is equipped with noters made of this material. Among the non-contact transducers (Fig. 39, pos. 5) converting the rotation rate to an electrical signal, the most widely used type is magnetic induction (Fig. 40). (Ivanova G.M. et al. 2005, 300.)

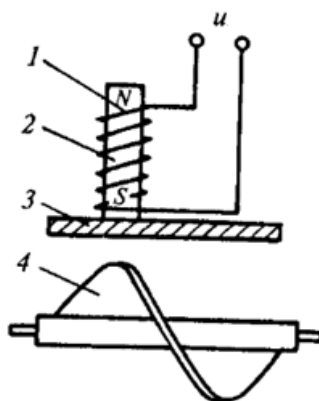


Figure 40. Scheme of the non-contact magnetic induction flowmeter. (Ivanova G.M. et al. 2005, 300.)

This transducer represents a coil *I* with a large number of turns, which is inserted into the magnet 2. The axes of the coil and the magnet are perpendicular to the axis of the non-magnetic tube 3. When impeller blades 4 (or a noter) pass by the magnet, a magnetic field changes causing the EMF pulse in the winding. It is obvious that the frequency of these pulses is equal to the number of revolutions of the impeller, multiplied by the number of blades. Impulse signal due to communication lines goes to the input of the measuring unit, which converts this signal into a current proportional to the flow rate. (Ivanova G.M. et al. 2005, 300-301.)

Ball-type flowmeter is a velocity flowmeter, in which a movable element is a ball continuously moving in the same plane on the inner surface of the pipe under the influence of pre-swirling flow. The velocity of the ball along the circumference of the pipe is proportional to the volumetric flow of liquid. Scheme of the ball-type flowmeter for medium and big flow rates is shown in Figure 41. Liquid flow, swirling by flow conditioner 1 in the helical direction, causes movement of the ball 2 around the circumference. For limiting the ball movement along the tube a limit ring 3 is installed, behind which a flow straightener 4 is located to straighten the swirling flow. On the outside of the nonmagnetic housing, a converter 5 converts the rotation rate of the ball to the frequency electrical signal. (Ivanova G.M. et al. 2005, 302.)

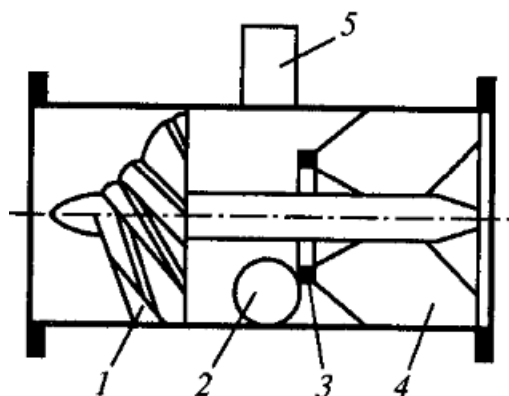


Figure 41. Ball-type flowmeter. (Ivanova G.M. et al. 2005, 302.)

Commercial ball-type flowmeters are used to measure the flow rate of liquids from 0.025 to 600 m³/h, at temperatures up to 285 °C and pressures up to 10 MPa. The density of the medium should be in the range of 700 ... 1400 kg/m³ and kinematic viscosity in the range (0,3 ... 12) · 10⁶ m²/s. (Ivanova G.M. et al. 2005, 303.)

4.4.3 Magnetic flowmeters

The operating principle of magnetic flowmeters is based on the law of electromagnetic induction, whereby in a conductive fluid intersecting a magnetic field an EMF is induced, proportional to the fluid velocity. Magnetic flow meters are designed to measure the flow rate of liquids with a conductivity is around 10 μS/cm. Currently, magnetic flowmeters are the most common devices for measuring the flow rate of water in pipes less than 250 mm. This is due to their positive features: readings do not depend on the viscosity and density of the medium, high dynamic range, flow transducers are inertialess, do not create pressure losses in the pipe, the impact of local resistance is much less than other flowmeters, so the required length of the straight sections is minimal, magnetic flowmeters are used in pipelines with a diameter from 2 to 4000 mm and can be used in cases where the use of other flowmeters is difficult or impossible.

The disadvantages of magnetic flowmeters include requirements for the minimum value of the electrical conductivity of the medium. Another disadvantage is a low level of primary

signal and the need of protection of the transducer and communication lines from external noise. (Ivanova G.M. et al. 2005, 305.)

Principle diagram of the magnetic flowmeter is shown in Figure 42. The working section of the pipe of the transducer 1 is made of non-magnetic material and covered inside with electrical insulation 2. This working section is located between the poles of an electromagnet. Electrodes 3 are passed through the wall of the pipe, which are in electrical contact with the liquid. The magnetic field lines are perpendicular to the plane through the axis of the pipe and to the line of electrodes. (Ivanova G.M. et al. 2005, 306.)

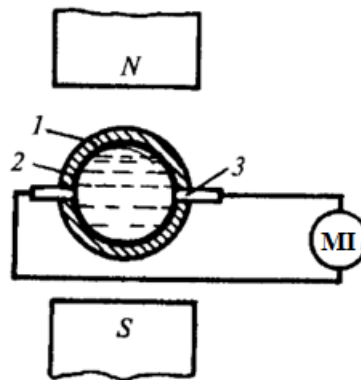


Figure 42. Magnetic flowmeter. (Ivanova G.M. et al. 2005, 306.)

In accordance with the law of electromagnetic induction, an asymmetric velocity profile in the fluid between the electrodes will induce an electromotive force

$$E = BDu, \quad (56)$$

where B - magnetic induction, u - average fluid velocity, D - diameter of the pipe.

Taking in to an account, that $u = 4G_0/(\pi D^2)$, we get:

$$E = 4BG_0/(\pi D), \quad (57)$$

where G_0 - volumetric flow rate. It follows that E is proportional to the volume flow rate. Measurement of the induced EMF is carried out with the measuring instrument MI. (Ivanova G.M. et al. 2005, 306.)

The use of permanent magnets minimizes external noise and increase the dynamic response of the device. However, a drawback is the polarization of the electrodes, which generates to a polarization voltage directed against the primary EMF.

To measure the flow of media with ionic conductivity flowmeter with an alternating magnetic field is applied (Fig. 43). When changing sinusoidal magnetic induction having B_m amplitude and frequency f , the expression for EMF looks

$$E = \frac{4G_0 B_m \sin(2\pi ft)}{\pi D}. \quad (58)$$

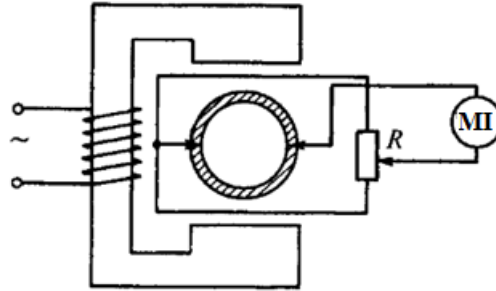


Figure 43. Magnetic flowmeter with alternating magnetic field. (Ivanova G.M. et al. 2005, 308.)

At a sufficiently high frequency f polarization of the electrodes is almost absent, however, the alternating magnetic field causes an erroneous EMF E_t . To eliminate this a phase shift of 90° between E and E_t is used. (Ivanova G.M. et al. 2005, 308.)

5 DESCRIPTIONS OF LABORATORY SESSIONS

This chapter provides a description of the two laboratory sessions, designed for an intensive course BH30A2200: “Experimental nuclear thermal hydraulics” in Lappeenranta University of Technology.

Two laboratory sessions should give students basic idea of measurements that are used in the industry and, in particular, in nuclear power engineering: temperature, pressure, pressure difference, liquid level in the tank and the flow rate measurements. In the laboratory exercises were restricted by maximum temperature (100 °C) and pressure (1 atm.). Because of these limitations a pressure measurement has no sense to be carried out, but measurement of the pressure difference is provided. Also, students are divided in to groups. There are three laboratory exercises. Two of them are about basic thermal hydraulics measurements and they are being developed in this work. The third laboratory exercise is the loop seal demonstration. Each group of students performs a separate laboratory exercise and has its own data for the calculation. Thus, every group does all different sessions in 3 days.

The equipment for the first lab exercise was created "from scratch" and demonstrates the natural circulation between the two vessels filled with water. The test rig is equipped to measure temperature, level and flow rate of the natural circulation.

An equipment for the second lab exercise is used to carry out measurements in pressure difference and the measuring of hydraulic losses in the pipe.

5.1 Laboratory session №1: Natural Circulation Test Rig

Natural Circulation Test Rig (NCTR) is presented in Figure 44.



Figure 44. Natural Circulation Test Rig.

thermocouples located on the surface of the tube 2: three on the hot (inner) side of the tube, two on the cold (outer) side at same heights as the two lower hot side TC:s and one on the bottom of the vessel near the intake of the pipe. The level of the liquid inside the tube 2 is measured by pressure difference transducer using a reference line 6. The reference line has a 2 kW heating element inside so that false level readings can be demonstrated.

Before laboratory work students must perform following preliminary tasks. It is allowed to use Internet, lectures and any other literature. Students are supposed to do this for three hours.

- What is a natural circulation and how is it formed?
- Find the correlation regarding calculation of natural circulation mass flow rate.
- Find the thermal conductivity equation for heat power (Fourier equation) in differential form and derive equation for cylindrical tube wall in integral form.
- Find the most common normalized signal ranges (A/V) of transducers used in automation. What are the advantages of (4 – 20 mA) signal?
- What are the functions of thermocouple wires? What are the properties of them?
- Using Figure 46, derive the equations: for fluid level $h_x(\Delta p_m)$ and for pressure difference $\Delta p_m(I)$. There is a linear dependency between Δp_m and electrical current signal (4 – 20 mA) so that $\Delta p_m = 0$ when $I = 4\text{mA}$ and $\Delta p_{max} = 50\text{kPa}$ when $I = 20\text{mA}$.
- Find a formula for absolute error of indirect measurements. Apply that formula for the obtained fluid level equation $h_x(\Delta p_m)$.

5.1.1 Level measurements

Laboratory work starts from water level measurement in the vessel. An assistant sets the valve position in accordance with the group number and switches on heating elements. As soon as water is heated up, level begins to rise. Level measurement is carried out with differential pressure gauge and reference line, which connected with gas part of the vessel.

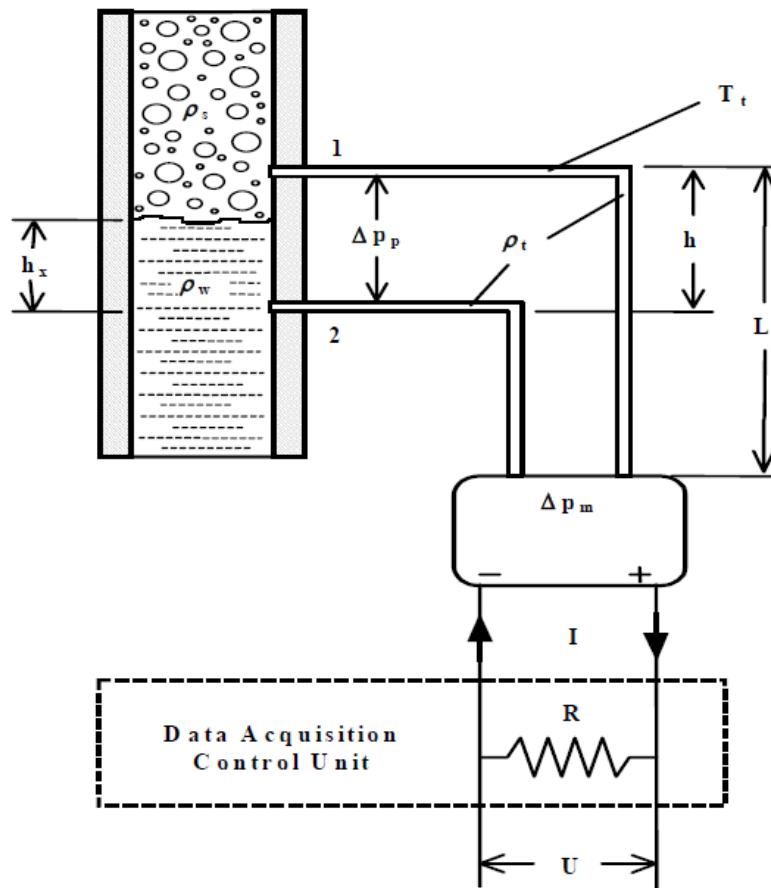


Figure 46. Fluid level measurement scheme. (Hyvärinen J. 2015, L11-12: 7.)

T_t	temperature of the fluid in the tap tubes	°C
ρ_t	average mass density of the fluid in the tap tubes	kg/m ³
ρ_w	average mass density of the fluid in the vessel	kg/m ³
ρ_s	average mass density of the air/steam mixture	kg/m ³
h	elevation distance between the two taps	m
L	elevation distance between the upper tap and the transducer	m
Δp_p	process pressure drop	Pa
Δp_m	measured pressure drop	Pa
I	transducer DC output current	A

Differential pressure transducer connected by taps 1 and 2 into the process plumbing provide the means for measuring total pressure drop across the taps. From total pressure drop, collapsed liquid level and void fraction can be calculated. The output of the

differential pressure transducers is an analog DC current between 4 mA and 20 mA which is converted to kPa units by the logic controller computer.

Foxboro differential pressure gauge with strain gauges is used (Fig. 47).



Figure 47. Differential pressure gauge Foxboro IDP-10. (Foxboro, 2015)

In the end of laboratory work students get a file in .lvm format with all the data of measurements. To calculate level of the vessel students will need values of densities, so they have to use values of temperatures, which also are being recorded during the exercise. Students should write down the times of actions taken during the experiment to ease searching of needed values in data file.

5.1.2 Temperature measurements

After the level measurements an assistant adds some water to the system to provide a natural circulation. Temperature measurements are conducted with six K-type thermocouples, which locations are shown in Figure 45. An output signal of thermocouple is a voltage $E(t, t_0)$ in volts (characteristic curve is presented in Figure 48).

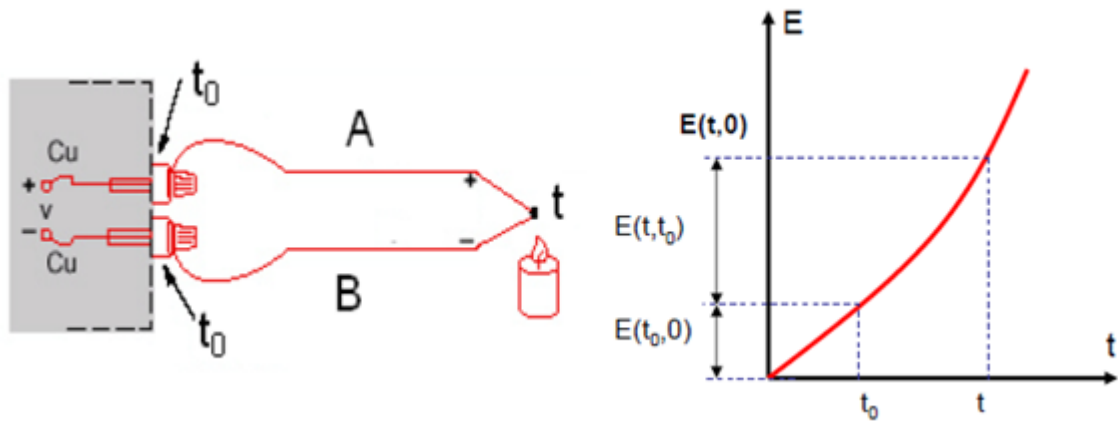


Figure 48. Characteristic curve of a thermocouple. (Tsypin A.V. 2011, 267.)

After natural circulation starts and readings of flowmeter appear students need to wait until circulation becomes stable and flow rate stabilizes. Students write down the time to conduct following calculations.

Students also have to take into account the cold junction temperature t_0 because it strongly impacts the calculations of the temperatures. In the data file they have this value in °C.

5.1.3 Flow rate measurements

Flow rate measurement is carried out with magnetic flowmeter Krohne Optiflux 4000 (Fig. 49). It has an output signal 4 – 20 mA, which is converted to m^3/s by the computer; students convert it to kg/s by multiplying it with density.

In the end of laboratory work an assistant switches on the heater installed inside reference line to demonstrate changes of level readings while actual level does not change.



Figure 49. Flowmeter Krohne Optiflux 4000. (Krohne, 2015)

5.1.4 Data processing

After performing the experiments students get their data file in .lvm form and use a spreadsheet program to make following calculation tasks:

Using the supplied equations and coefficients from IST-90 tables the temperature measurements have to be converted from Volts to Celsius. It should be noted, that equations use mVs whereas the measurement system uses Volts.

Using the equation derived in preliminary exercise students calculate the fluid level h_x in meters. There is a linear dependency between Δp_m and electrical current signal (4 – 20 mA) so that $\Delta p_m = 0$ when $I = 4$ mA and $\Delta p_{max} = 15$ kPa when $I = 20$ mA. Density ρ_s should be assumed as a density of 100 % moist air at the temperature of water surface.

Calculation of the natural circulation mass flow rate is done with the equation found the in preliminary task. According to a group number of a student, a friction factor is chosen from the table 1. Calculated and measured values are compared.

Table 1. Friction factor.

№	1	2	3
Friction factor, F	1961	3097	9807

Estimation of an average thermal power transferred through the wall is performed using Fourier equation for cylindrical wall. Because thermocouples measure water temperature near the wall of the tube, wall temperatures are assumed to be approximately equal to water temperatures. The wall is made of polycarbonate.

Last task is to calculate an error estimation of level measurement using equation derived in a preliminary exercise. The error assumption of water height determination in reference line is 1% of measured value. It should be taken in to an account, that temperature measurement accuracy impacts an error of densities. The error of pressure difference determination is combined from errors of the d/p transmitter and analog current input module cFP-AI-111. All the necessary values are present in additional specification sheets of d/p transmitter and cFP-AI-111.

5.1.5 Friction factor calculation

Each group performs laboratory work with different valve position. One group makes experiments with fully opened valve, other groups make with partly closed. But for some calculation tasks a friction factor value is needed. To determine this value additional experiments were carried out while preparing the laboratory session. For all three positions of the valve, the rig was filled with water. Because of the different hydraulic resistances water levels in the vessel and in the plastic tube were different. This difference and the flow rate were measured.

$$\text{Level difference} \quad \Delta h = \begin{pmatrix} 7 \\ 10 \\ 25 \end{pmatrix} \text{ mm;}$$

$$\text{Volumetric flow rate} \quad G = \begin{pmatrix} 2.1 \\ 1.9 \\ 1.5 \end{pmatrix} \text{ l/s;}$$

Because the flow is laminar inside the channel next formulas are applied (Hyvärinen J. 2015, L9-10: 21.):

$$R = \frac{\Delta h g \rho}{1/2 \rho^{-1} (G \rho)^1};$$

Friction factor

$$F = \frac{R}{2\rho} = \left(\frac{1961}{3097} \right);$$

Obtaining friction factor is necessary for natural circulation mass flow rate calculation:

$$q_m = \left(\frac{\rho_{av} \beta Q_{heat} g H}{F c_p} \right)^{1/2};$$

where:

$$\rho_{av} = \frac{\rho_h + \rho_c}{2} \quad \text{an average density of water;}$$

$$\beta = \frac{|\rho_h - \rho_c|}{\rho_{av} \Delta T} \quad \text{an expansion coefficient;}$$

$$Q_{heat} \quad \text{a power of electrical heaters;}$$

$$F \quad \text{friction factor.}$$

Water temperatures of hot and cold sides are determined as a weighted average between thermocouple readings.

5.2 Laboratory session №2: Horizontal and Inclined Pipe flow Experiments

The equipment for Horizontal and Inclined Pipe flow Experiments (HIPE) is shown in Figure 50.



Figure 50. Horizontal and Inclined Pipe flow Experiments facility.

Two-phase flow test facility was constructed to study the applicability of Particle Image Velocimetry (PIV) and Wire-Mesh Sensors (WMS) for different types of single- and two-phase flows. Test facility was designed in such a way that it enables experiments at any inclination of the flow channel, hence the name HIPE (=Horizontal and Inclined Pipe flow Experiments). Test facility is also used for demonstrational and educational purposes. (LUT. HIPE Test Facility.)

Test section is equipped with in-house manufactured WMSs (32×32 wires). The sensors are recording the flow at 5000 fps. In addition, a special channel section was designed and constructed that enables High-Speed Camera (HSC) and PIV measurements by minimizing the optical distortions. The facility is equipped with a magnetic flowmeter and differential pressure gauges. Some parameters of the test facility are summarized into the table 2. (LUT. HIPE Test Facility.)

Table 2. Facility parameters. (LUT. HIPE Test Facility.)

Inside / Outside diameter of the flow channel	50 mm / 60 mm
Inside / Outside diameter of narrow the flow channel	30 mm / 40 mm
Inclination of the flow channel (from horizontal)	0°- 90°
Material of the flow channel	PMMA
Pressure / Temperature	Atmospheric
Flow types	Water / Air-Water

5.2.1 Preliminary exercises

- Find the equation for pressure losses inside the channel of one-phase flow.
- Find the equation for local pressure losses of one-phase flow (sudden contractions, expansions).

- Find correlations for two-phase friction multipliers from a) Martinelli-Nelson, b) Baroczy to calculate pressure loss.
- Find correlations for local pressure losses of two-phase flow (sudden contractions, expansions).
- Find correlation for slip ratio estimation.

5.2.2 Performance

Channel consists of a pipe with inner diameter of 50 mm connected to a pipe with inner diameter of 30 mm and length of 935 mm and then again with 50 mm pipe. Flowing through the channel is water or water/air mixture that experiences several resistances: a sudden contraction, a wall friction and a sudden expansion. D/p transmitter measures pressure difference over the narrow part of the channel.

To perform lab work students have to plan experimental points. To do that they should choose from table ranges of water and air mass flow rates in accordance with their group number. There are eight experiments that have to be carried out: three of single-phase (water) experiments and five of two-phase experiments (air/water mixture).

Preliminary experiments showed that for a stable operation of the facility, experimental points must be within ranges presented in the table 3.

Table 3. Mass flow rates ranges.

№	1	2	3
Water mass flow rate, kg/s	1.2 - 2	2 – 2.8	2.8 – 3.6
Air mass flow rate, g/s	0.5 – 2	0.5 – 2	0.5 – 2

After students have planned measurements, the assistant adjusts the mass flow rates on the facility. Time of each experiment is written down for easy searching of the certain experiment in the data file, which students get in the end of laboratory exercise.

5.2.3 Data processing

After performing the experiments students make following calculations:

- Using equations found in preliminary exercise calculate pressure losses over the channel for water flow. Compare calculated values with measured ones.
- Using Martinelli-Nelson correlation found in preliminary exercise calculate pressure losses over the channel for air/water flow. Compare calculated values with measured.
- Using Baroczy correlation found in preliminary exercise calculate pressure losses over the channel for air/water flow. Compare calculated values with measured.

6 SUMMARY

In this master's thesis light water reactors and their components are described. Also advantages and disadvantages of light water reactors and water as a coolant and moderator are explained.

Second chapter presents all main phenomena that exist in the primary circuit of light water reactors in normal and abnormal conditions: natural circulation, forced convection, one-phase and two-phase friction, critical flow, flooding, boiling and condensation. These phenomena have to be controlled and this control is provided with measurement and control instruments.

All basic thermal hydraulics measurement techniques are described in details: temperature, pressure, pressure difference, fluid level and flow rate. Temperature measurement instruments are presented by copper and platinum resistance thermometers and thermocouples. Pressure and pressure difference measurements are conducted in NPPs with piezoelectric converters, piezoresistive strain gauge and capacitive pressure sensors. Main level measurement techniques contain D/p level transmitters, float level indicators, buoyancy level transmitter and capacitive level indicator. Flow rate in NPPs is measured using variable-pressure drop method, velocity flowmeters and magnetic flowmeters.

The result of this work is a development of laboratory exercises for basic nuclear thermal hydraulics measurements. Laboratory sessions are developed for students of Lappeenranta University of Technology who have bachelor status. These exercises were presented as a part of intensive course BH30A2200 "Experimental nuclear thermal hydraulics" in school of Energy Systems.

References

BOBROVNIKOV G.N., KATKOV A.G., 1977. Level measurement techniques. Mashinostroenie. 165 p. (in Russian).

CHERUBINI M., GIANNOTTI W., ARANEO D., D'AURIA F., 2007. Use of the Natural Circulation Flow Map for Natural Circulation Systems Evaluation. University of Pisa. Pisa, Italy.

DEREVYANKO O.V., KOROLEV A.V., POGOSOV A.Y., 2014. Pre-alarm physical processes and sustainable heat removal in nuclear engineering power systems. Odessa, Ukraine. 264 p. (in Russian).

FOXBORO. 2015. PSS 2A-1C14B. Field devices – pressure, product specifications. [Accessed on 08.2015].

Available at: http://resource.invensys.com/instrumentation/documentation/eib/pss/pss_2a-1c14b.pdf

GERLAND W.A., GANIC E.N. 2005. Flooding in counter-current two-phase flow. Illinois, USA.

GHIAASIAAN S.M., 2007. Two-Phase Flow, Boiling, and Condensation: In Conventional and Miniature Systems. Cambridge University Press. New York, USA. 636 p.

GONEK N.F., 1979. Pressure gauges. Mashinostroenie. Leningrad, Soviet Union. 174 p. (in Russian).

GORDOV A.N., ZHAGULLO O.M., IVANOVA A.G., 1992. Basics of temperature measurements. Energoatomizdat. Moscow, 304 p.

LUT. 2014. HIPE Test Facility. [Accessed on 03.2015] Available at: <https://ydin.pc.lut.fi/EDS/Public/General/hipe/>

HYVÄRINEN J., 2015. Lecture course: BH30A1900 Thermal Hydraulics of Nuclear Power Plants. Lappeenranta University of Technology. Lappeenranta, Finland.

HYVÄRINEN J., 2015. Lecture course: BH30A2200 Experimental Thermal Hydraulics of Nuclear Power Plants. Lappeenranta University of Technology. Lappeenranta, Finland.

ISACHENKO V.P., OSIPOVA V.A., SUKOMEL A.S., 1975. Heat transfer. Energia. Moscow, Russia. 488 p. (in Russian).

IVANOVA, G.M., KUZNETSOV N.D., CHISTYAKOV V.S., 2005. Thermotechnical measurements and instrumentation. Moscow Power-Engineering Institute. Moscow, Russia. 460 p. (in Russian).

KOROTKIKH A.G., SHAMANIN I.V., 2007. Basics of hydrodynamic and heat transfer in nuclear reactors. Tomsk State University. Tomsk, Russia. 117 p. (in Russian).

KROHNE. 2015. Electromagnetic flowmeters – OPTIFLUX 4000 Sensor. [Accessed on 08.2015]. Available at: <http://krohne.com/en/products/flow-measurement/electromagnetic-flowmeters/sensors/optiflux-4000/>

KREMLEVSKIY P.P., 1989. Flow meters and totalizers. Mashinostroenie. Leningrad, 775 p. (in Russian)

LABUNTSOV D.A., 2000. Physical basics of power-engineering. Moscow Power-Engineering Institute. Moscow, Russia. 388 p. (in Russian).

LABUNTSOV D.A., YAGOV V.V., 2000. Mechanics of two-phase systems. Moscow Power-Engineering Institute. Moscow, Russia. 374 p. (in Russian).

LAMARSH J.R., BARATTA A.J., 2001. Introduction to Nuclear Engineering. Pearson. 744 p.

LYSIKOV B.V., PROZOROV V.K., 1980. Reactor thermometry. Atomizdat. Moscow, 199 p. (in Russian).

NAGAE T., MURASE M., WU T. and VIEROW K., 2005. Evaluation of Reflux Condensation Heat Transfer of Steam – Air Mixtures under Gas-Liquid Countercurrent Flow in a Vertical Tube. Journal of nuclear science and technology. USA. 50-57 p.

TONG L.S., SIDOROV V.Y., 1969. Boiling heat transfer and two-phase flow. Mir. Moscow. (in Russian).

TSYPIN A.V., 2011. Lecture course: Metrology. Moscow-Power engineering Institute. Muscow, Russia. (in Russian).

VIDYAEV D.G., 2009. Fluid dynamics. Tomskiy Politehnicheskij University. Tomsk. Russia. 108 p. (in Russian).

ZOHURI B., FATHI N., 2015. Thermal-Hydraulic Analysis of Nuclear Reactors. Springer. New Mexico, USA.

Study guidance of natural circulation test rig laboratory session



LUT

Lappeenranta

University of Technology

LUT School of Energy Systems

BH30A2200 Experimental Nuclear Thermal Hydraulics

**NATURAL CIRCULATION TEST RIG
LABORATORY SESSION**

The goal of work is to familiarize students with basic measurements that are used in industry and, particularly, in nuclear power plants; obtaining skills in converting transducer's signal into quantity of interest; estimation of the error of the measurements.

Facility description.

Principle scheme of Natural Circulation Test Rig (NCTR) and its dimensions are shown in figure 1.

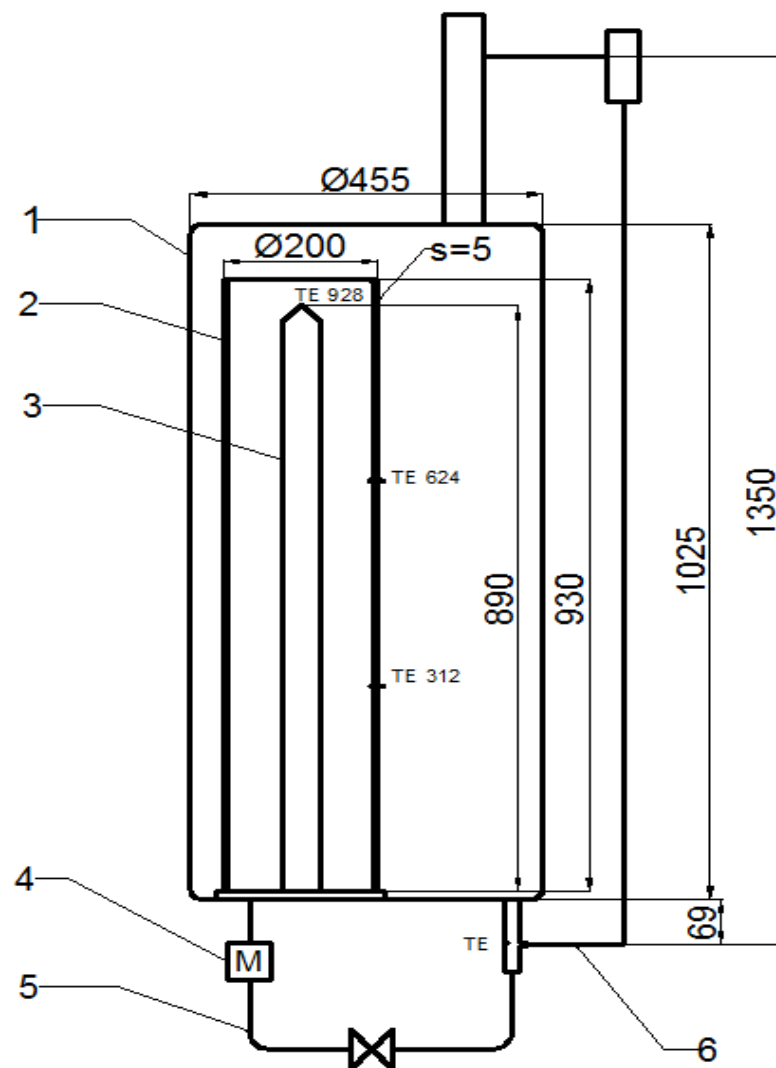


Figure 1. Principle scheme of Natural Circulation Test Rig

NCTR represents the glass vessel 1 with inner tube 2 made of polycarbonate. They are connected with a pipe 5 located under the vessel. This system of communicating vessels is filled with water. Inside the tube 2 there are six heating elements 3 with maximum combined power 13,23 kW. When heating elements heat up the water inside the tube, warm water rises to the upper part of the tube and eventually flows over into the cold side. Cold water comes from the main vessel through the pipe 5 where the flow is measured using a magnetic flow meter 4. The temperature is measured with six K-type thermocouples located on the surface of the tube 2: three on the hot (inner) side of the tube, two on the cold (outer) side at same heights as the two lower hot side TC:s and one on the bottom of the vessel near the intake of the pipe. The level of the liquid inside the tube 2 is measured by pressure difference transducer using a reference line 6. The reference line has a 2 kW heating element inside so that false level readings can be demonstrated.

Preliminary exercise

Before performing the lab work complete following tasks. You can use Internet, lectures or any other literature.

- What is a natural circulation and how is it formed?
- Find the correlation regarding calculation of natural circulation mass flow rate.
- Find the thermal conductivity equation for heat power (Fourier equation) in differential form and derive equation for cylindrical tube wall in integral form.
- Find the most common normalized signal ranges (A/V) of transducers used in automation. What are the advantages of 4 – 20 mA signal?
- What are the functions of thermocouple wires? What are their properties?
- Using figure 2 and a general equation for collapsed level from lecture, derive the equation for fluid level $h_x(\Delta p_m)$. Use a substitution $\rho_{t_1}L = \rho_{t_1}h + \rho_{t_2}(L - h)$ as in this way the heated part of the tap 1 is considered correctly.
- Use the error propagation law to find a formula for error estimation for the obtained fluid level equation $h_x(I)$.

Fluid level measurement

Fluid level measurements are conducted by differential pressure transducer and a reference line. Principle of the scheme is shown in figure 2.

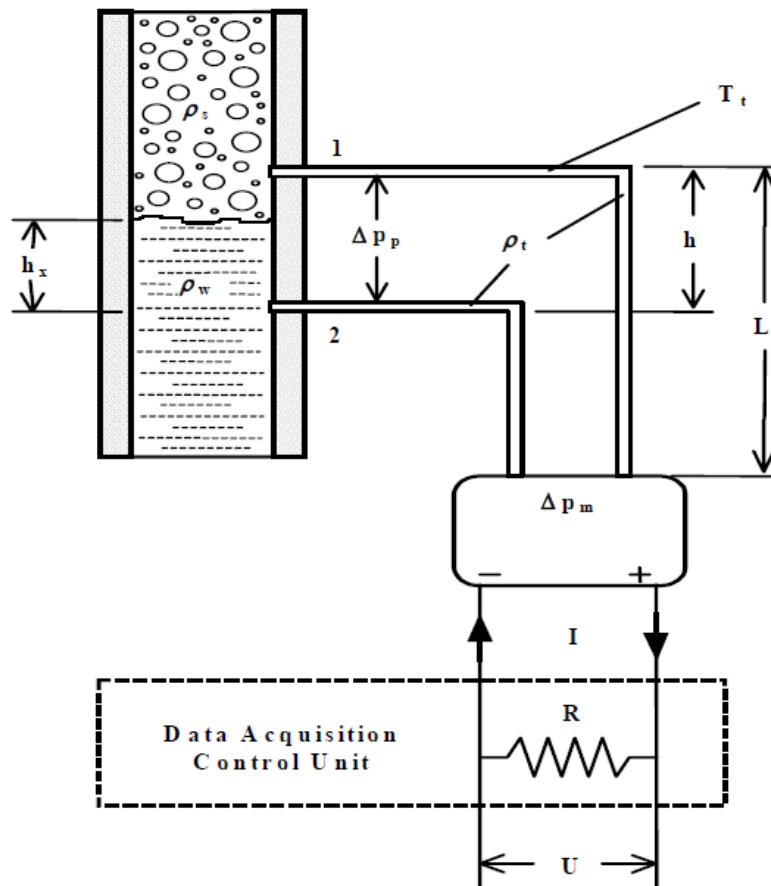


Figure 2. Fluid level measurement scheme

T_t	temperature of the fluid in the tap tubes	°C
ρ_t	average mass density of the fluid in the tap tubes	kg/m ³
ρ_w	average mass density of the fluid in the vessel	kg/m ³
ρ_s	average mass density of the air/steam mixture	kg/m ³
h	elevation distance between the two taps	m
L	elevation distance between the upper tap and the transducer	m
Δp_p	process pressure drop	Pa
Δp_m	measured pressure drop	Pa
I	transducer DC output current	A

Differential pressure transducer connected by taps 1 and 2 into the process plumbing provide the means for measuring total pressure drop across the taps. From total pressure drop, collapsed liquid level and void fraction can be calculated. The output of the differential pressure transducers is an analog DC current between 4mA and 20 mA which is converted to kPa units by the computer though recorded in mAs.

Temperature measurement

Temperature measurements are conducted with 6 K-type thermocouples. Three thermocouples are installed on the inner surface of the tube and measure hot water temperature. Two thermocouples are installed on the outer surface of that tube and measure cold water temperature. And one thermocouple is installed at the bottom of the main vessel. Elevation values are shown in figure 1. Output signal of thermocouples is a voltage.

Mass flow rate measurement

Mass flow rate measurements are performed with magnetic flowmeter. The flowmeter measures natural circulation mass flow rate. Output signal is in mA which is converted to m³/s by the computer.

Performance

After switching on the heaters, water will be heated up and water level inside the tube will start rising. When the assistant tells you, write down the time from the screen. It is needed

in the post-processing phase of the experiment when searching for the correct data points from the file, which will be given to you after the lab work has been accomplishment.

After water level measurements some water must be added to the system to provide natural circulation. In accordance with your group number, an assistant sets the valve position to change a hydraulic resistance. During heating up wait until a stable mass flow rate will appear. Write down the time from the screen as this is the beginning of the natural circulation for your group.

In the reference line a 2 kW heater is installed to demonstrate that density of water in reference line affects fluid level readings. Remember that after this demonstration the level measurements no longer give out correct levels.

Data processing

You will be given a data file with all recorded measurements in .lvm form. When importing the file, make sure the measurement channels are distributed correctly in to separate columns. The columns in the file are tab-delimited and can be opened in Excel. Find values according to the time you wrote down during the experiment and write out them to a new Excel sheet.

- Using the supplied equations and coefficients from http://srdata.nist.gov/its90/type_k/kcoefficients_inverse.html and http://srdata.nist.gov/its90/type_k/kcoefficients.html convert the temperature measurements from Volts to Celsius. Notice that equations use mVs.
- Using the equation derived in preliminary exercise calculate the fluid level h_x in meters. There is a linear dependency between Δp_m and electrical current signal (4 – 20 mA) so that $\Delta p_m = 0$ when $I = 4\text{mA}$ and $\Delta p_{max} = 15\text{ kPa}$ when $I = 20\text{ mA}$. Assume that ρ_s is a density of 100 % moist air at the temperature of the water surface.
- Calculate a natural circulation mass flow rate with the equation found the in pre-task. According to your group number choose a friction factor from the table below. Compare calculated values with measured.

№	1	2	3
Friction factor, F	1961	3097	9807

- Estimate an average heat power transferred through the wall using Fourier equation for cylindrical wall. Assume that wall temperatures are equal to water temperatures. The wall is made of polycarbonate. Would it be possible to achieve natural circulation if tube was made of copper?
- Calculate an error estimation of level measurement using equation derived in pre-exercise. Assume that error of water height determination in reference line is 1% of measured value (figure 1). An error of densities $\Delta\rho$ is dependent on the temperature measurement accuracy. The error of pressure difference determination Δp_m is calculated comparable to the earlier calculation exercise and it is combined from errors of the d/p transmitter and analog current input module cFP-AI-111. In additional specification sheets for d/p transmitter, find the values of error for span code C. Remember that d/p transmitter has analog linear output. From cFP-AI-111 specification calculate its error that consists of nonlinearity, offset error and gain error.

Study guidance of Horizontal and Inclined Pipe flow experiments laboratory session



LUT

Lappeenranta

University of Technology

LUT School of Energy Systems

BH30A2200 Experimental Nuclear Thermal Hydraulics

**HORIZONTAL AND INCLINED PIPE FLOW
EXPERIMENTS
LABORATORY SESSION**

The goal of this work is to test pressure loss correlations for one and two-phase flows by comparing calculated values of pressure losses with measured pressure difference.

Facility description

Two-phase flow test facility was constructed to study the applicability of Particle Image Velocimetry (PIV) and Wire-Mesh Sensors (WMS) for different types of single- and two-phase flows. Test facility was designed in such a way that it enables to conduct experiments at any inclination of the flow channel, hence the name. HIPE (=Horizontal and Inclined Pipe flow Experiments) test facility offers many possibilities to study and measure flow transitions at different inclinations. Test facility is also used for demonstrational and educational purposes.

Test section is equipped with in-house manufactured WMSs (32×32 wires). The sensors are recording the flow at 5000 frames/s. In addition, a special channel section was designed and constructed that enables High-Speed Camera (HSC) and PIV measurements by minimizing the optical distortions. Some parameters of the test facility are summarized into the table.

Table 1. Facility parameters

Inside / Outside diameter of flow channel	50 mm / 60 mm
Inside / Outside diameter of narrow flow channel	30 mm / 40 mm
Inclination of the flow channel (from horizontal)	0°- 90°
Material of the flow channel	PMMA
Pressure / Temperature	Atmospheric
Flow types	Water / Air-Water

Preliminary exercise

Before performing the lab work complete following tasks. You can use Internet, lectures or any other literature.

- Find the equation for pressure losses inside the channel of one-phase flow.
- Find the equation for local pressure losses of one-phase flow (sudden contractions, expansions).
- Find correlations for two-phase friction multipliers from a) Martinelli-Nelson, b) Baroczy to calculate pressure loss.
- Find correlations for local pressure losses of two-phase flow (sudden contractions, expansions).
- Find correlation for slip ratio estimation.

Performance

Channel consists of a pipe with inner diameter 50mm connected with a pipe with inner diameter 30mm and length 935mm and then again with 50mm pipe. Flowing through the channel water or water/air mixture experiences several resistances: a sudden contraction, a wall friction and a sudden expansion. D/p transmitter measures pressure difference over the narrow channel.

To perform lab work make a plan of your experiments: choose from table below ranges of water and air mass flow rates in accordance with your group number. You have to conduct 8 experiments: 3 single-phase (water) experiments and 5 two-phase experiments (air/water). Write down 8 points that you have chosen.

№	1	2	3
Water mass flow rate, kg/s	1.2 - 2	2 – 2.8	2.8 – 3.6
Air mass flow rate, g/s	0.5 – 2	0.5 – 2	0.5 – 2

Tell the assistant your plan of the measurements. After he sets the mass flow rates on the facility, write down the time of each experiment for searching of the certain experiment from a data file. Do all 8 measurements accordingly.

Data processing

You will be given data file in .lvm form with all recorded measurements. This file can be opened in Excel. Find values according to the time and copy them to a new Excel file.

- Using equations found in preliminary exercise calculate pressure losses over the channel for water flow. Compare calculated values with measured ones.
- Using Martinelli-Nelson correlation found in preliminary exercise calculate pressure losses over the channel for air/water flow. Compare calculated values with measured.
- Using Baroczy correlation found in preliminary exercise calculate pressure losses over the channel for air/water flow. Compare calculated values with measured.